On the Interactions between Large-Scale Structure and Fine-Grained Turbulence in a Free Shear Flow. III. A Numerical Solution

T. B. Gatski and J. T. C. Liu

Email alerting service	Receive free email alerts when new articles cite this article - sign up in the box at the top right-hand corner of the article or click **here**

To subscribe to *Phil. Trans. R. Soc. Lond. A* go to: **http://rsta.royalsocietypublishing.org/subscriptions**

[473]

ON THE INTERACTIONS BETWEEN LARGE-SCALE STRUCTURE AND FINE-GRAINED TURBULENCE IN A FREE SHEAR FLOW. III. A NUMERICAL SOLUTION†

BY T. B. GATSKI‡ AND J. T. C. LIU‖

Division of Engineering, Brown University, Providence,
Rhode Island 02912, U.S.A.

CONTENTS

We present the results of a numerical computation of the interactions between the horizontally periodic monochromatic component of a large-scale coherent structure and the fine-grained turbulence in a mixing layer. The dependent variable characterizing the coherent structure is the *total* flow quantity which includes both the Reynolds-averaged (here the horizontal average) mean flow and the large-scale coherent structure, this being distinguished from the fine-grained turbulence by a

conditional average linked to the periodicity of the coherent structure. The dependent variables characterizing the fine-grained turbulence are the conditionally averaged turbulent stresses, which are themselves *total* quantities comprising the Reynolds-averaged mean stresses and the coherent-structure induced or modulated stresses. The transport equations for such conditionally averaged quantities are identical in form to the Reynolds-mean equations. Closure approximations for the Reynolds-mean stresses due to Launder *et al.* (1975) are directly extended to the conditionally averaged stresses. These approximations include the pressure–velocity strain redistribution which accounts for rapid distortions due to the large-scale coherent structure, a simple diffusional approximation to the triple correlations and an approximate transport equation for the rate of viscous dissipation. The large-scale structure is two dimensional with its vorticity axis perpendicular to the mean flow direction, the fine-grained turbulence being three dimensional. The initial conditions are made self-consistent by numerically solving the horizontally homogeneous, time-dependent, Reynolds-mean problem in the absence of coherent structure until the mean Reynolds stresses and viscous dissipation become self-similar as the shear layer growth rate becomes constant. The solution to the Rayleigh equation with this self-similar mean velocity profile is then obtained. The wavenumber mode which corresponds to the most-amplified case is then *suddenly* imposed, together with the Reynolds mean velocity, as the initial condition for the large-scale structure. It is argued that, since the coherent structure-induced stresses and viscous dissipation function develop in finite time, the initial conditions for the conditionally averaged turbulence quantities are precisely those for the initial self-similar Reynolds-mean quantities, consistent with the sudden imposition of a large-scale structure upon the flow. The structural details are presented in terms of the time evolution of the conditionally averaged streamfunction and vorticity contours. While the streamline patterns resemble Kelvin's cats' eyes, the vorticity patterns display large non-uniformities within the cats' eyes; thus it is not possible to construct an analytical nonlinear critical layer theory for this problem consistent with the numerical results. The physical interpretation is presented, after Reynolds (horizontal) averaging, in terms of the time evolution of global energy-exchange mechanisms between the Reynolds-averaged mean flow, the large-scale coherent structure and the fine-grained turbulence. The mean flow loses energy to both components of the oscillations, the large-scale structure gains energy from the mean flow and loses energy to the fine-grained turbulence, and the fine-grained turbulence gains energy from both the mean flow and the large-scale structure and loses kinetic energy through viscous dissipation of the small eddies. The possibility that the large-scale structure transfers energy back to the mean flow (like 'damped' disturbances in hydrodynamic stability interpretations) is also shown. Owing to the nonlinear interaction between the mean flow and large-scale structure, through the action of the large-scale Reynolds stresses, the global energy of the large-scale structure first increases and then decays with time. Such a growth and decay reflects the inability, at some time, of the large-scale to effectively transfer energy from the mean flow and to subsequently transfer energy back to the mean flow through the action of the large-scale Reynolds stresses. The simultaneous evolution of the global fine-grained turbulent energy exhibits an increase from its initial self-preservation level to a final, higher one, in response to the new mean flow condition caused by the evolution of the large-scale structure. This physical picture of the global energy evolution is consistent with previous much-simplified analyses of the temporal problem (Liu & Merkine 1976 *a*) and approximately consistent with results for the spatial problem as well (Alper & Liu 1978). The structural details of the direct production mechanisms of the conditionally averaged horizontal and vertical contributions to the fine-grained turbulence energy from the two dimensional, large-scale structure are shown in terms of contour plots for the cats' eyes regions; of these, the dominant production mechanisms essentially resemble the contours of the horizontal and vertical contributions to the turbulence energy. Since there is no direct production mechanism for the spanwise contribution to the turbulence energy, this contribution must arise entirely from the pressure–velocity strain redistribution mechanism obtained from the closure approximation. The

structural details of this redistribution mechanism essentially resemble those of the span-wise contribution to the turbulence energy. Certain apsects of available experimental observations are interpreted in terms of the present considerations. Finally, the importance of well-controlled experiments to further study the large-scale coherent structures in free turbulent shear flows is re-emphasized.

1. Introduction

The interactions between a monochromatic component of the large-scale coherent structure and fine-grained turbulence in developing mean flows with inflexional profiles have recently been analyzed (Liu & Merkine 1976a; Liu & Alper 1977; Liu et al. 1977; Alper & Liu 1978). There, ideas from nonlinear hydrodynamic stability theory (Stuart 1958; Liu 1971) are utilized to obtain the 'amplitude' equations for the mean flow, the large-scale coherent structure and the disparately fine-grained turbulence from their respective kinetic energy equations. The nonlinear interactions between the three components of flow are depicted in terms of the non-equilibrium adjustments between the mean shear layer growth rate and the integrated energy densities of the large-scale structure and the fine-grained turbulence. It is interesting to note that imposing an initially most-amplified mode of the large-scale structure on the flow gives a spatial spreading rate for the equilibrium shear layer of about 0.14–0.17 from approximate considerations (Alper & Liu 1978), while observations of Liepmann & Laufer (1947) give 0.16. The most interesting events occur in the non-equilibrium adjustment region: here the large-scale structure amplifies owing to energy production from the mean flow and subsequently decays owing to energy transfer to the fine-grained turbulence. The fine-grained turbulence adjusts from its initial level to a new higher kinetic energy level by extracting energy from the large-scale structure, energy production from the mean and the rate of viscous dissipation play the usual familiar role. A similar picture of the life cycle of a non-equilibrium adjustment event has in fact been obtained in experimental observations, and there too the large-scale structure is explicitly educed from the total fluctuations; it is thus possible to study the process of energy cascading from a single mode of large-scale coherent structure to the rest of the disparately fine-grained random turbulence (Binder & Favre-Marinet 1973; Favre-Marinet 1975).

Although some of the overall features of observations can be explained via the approximate energy integral considerations described above, such methods cannot always provide the details of the local structures involved. This is not unlike the situation in laminar flows, where the extension of Stuart's (1958) ideas to the approximate description of the interactions between developing mean flows and nonlinear instabilities has achieved some measure of success in comparison with experiments (Ko et al. 1970; Liu & Lees 1970; Liu & Gururaj 1974; Liu & Merkine 1976b). Complementing such nonlinear hydrodynamic stability analyses are numerical solutions of the finite-amplitude instabilities with the full unsteady Navier–Stokes equations in a laminar flow found in the works of Amsden & Harlow (1964) and Patnaik et al. (1976). There the appropriate dependent variable is the total flow quantity rather than its two components, the mean flow and the instability. The two components of the flow as well as their mutual inter-actions can always be obtained from the numerical solution by appropriate averaging. The prospects of applying such numerical methods to the dynamical equations in order to obtain the large-scale coherent structure in turbulent shear flows are discussed in Liu & Alper (1977) and Liu et al. (1977). The present paper presents the numerical results of such an approach and analyses, in particular, the interaction of an initially monochromatic component of the

large-scale coherent structure with the fine-grained turbulence in a temporal mixing layer of horizontally homogeneous and oppositely directed streams. The large-scale coherent structure is horizontally periodic and develops in time. The physical significance of this problem is that it strongly resembles (though does not exactly correspond to) the spatially developing free shear layer observed in laboratories. The coherence or periodicity enters into the horizontal boundary conditions and the numerical problem is well defined. On the other hand, the numerical problem for the spatially developing free shear layer is not well defined because of the necessary but unknown boundary conditions downstream.

In the previous approximate analyses (Liu & Merkine 1976a; Alper & Liu 1978) the flow quantity was split into three components following Reynolds & Hussain (1972): a mean flow, a large-scale coherent structure and a fine-grained turbulence component. There, two averaging procedures are necessary to consider the interaction among the three components of flow: the conditional average, in particular the phase average, which explicitly educes the coherent structure from the total fluctuations containing both random and coherent components; and the usual Reynolds average which sorts out the fluctuations from the mean. In the present numerical scheme, the appropriate dependent variable is one which comprises both the mean and the large-scale coherent structure. The dynamical equations obtained for such a total 'coherent structure' quantity are identical to the unsteady equations for the 'mean' quantities in the Reynolds sense, except that the fine-grained turbulent stresses are now interpreted as being conditionally averaged (not, as is usual, Reynolds-averaged). The conditionally averaged stresses, like the dependent dynamical variables characterizing the coherent structure, consist of a mean part, which is in fact the Reynolds or the mean stress, and a coherent-structure-induced stress which has the same periodicity as the coherent structure. The dynamical equations for the large-scale coherent structure is augmented by the conservation equations for the conditionally averaged fine-grained turbulent stresses which must be closed. Closure is obtained here by a direct extension of the Launder *et al.* (1975) model to the problem of the conditionally-averaged stresses. It is, of course, difficult to justify a direct extension of closure schemes for mean stresses to conditionally averaged stresses. However, this direct extension is accepted here by way of assumption about the conditionally averaged fine-grained turbulence quantities with which the large-scale coherent structure interacts. It is most probably immaterial which of the available higher-order closure schemes for the mean stresses is used for such an extension, since the central problem is still the large-scale structure. Launder's model is chosen, however, because it will result in the fewest assumptions about the direction of energy transfer between the disparate scales of motion. We have left this issue to careful but approximate calculations, rather than to assumption, in the integral energy considerations (Liu & Merkine 1976a; Liu & Alper 1977; Alper & Liu 1978).

2. Formulation of the problem

In contrast to our previous *approximate* analyses (Liu & Merkine 1976a; Liu & Alper 1977; Alper & Liu 1978) in which the flow quantities were split into three components (Reynolds & Hussain 1972), the mean flow, the large-scale structure and the fine-grained turbulence, the present *computational* problem necessitates a splitting into only two components: a coherent part (which includes both the mean flow and the large-scale structure) and the fine-grained turbulence. Mean quantities are obtainable from the numerical results by horizontal averaging, as are the interaction mechanisms in the mean. Thus neither prior horizontal averages nor mean

quantities are explicitly involved in the computational scheme. Only the conditional average (which is here the phase average), linked to the horizontal periodicity of the large-scale structure, is involved in the extraction of our 'proper' dynamical dependent variable from the fine-grained turbulence.

(a) Conservation equations

In the following, the velocity components and coordinates are made dimensionless by the free stream velocity and the initial shear layer thickness, respectively; the pressure is made dimensionless by the free-stream dynamic pressure, and the time by the free stream velocity and the initial shear layer thickness. We shall denote the conditional average by $\langle\ (\ )\ \rangle$ and the horizontal average, to be used after the numerical results have been obtained for diagnostic purposes, by $(\ \bar{}\ )$. The dynamical dependent variables, velocity and pressure, are denoted by the script symbols

$$U_i(x_i, t) = \bar{U}_i(x_i, t) + \tilde{u}_i(x_i, t), \quad P(x_i, t) = \bar{P}(x_i, t) + \tilde{p}(x_i, t),$$

respectively; the mean flow is denoted by an overbar, the large-scale structure identified by a tilde ($\sim$) and the fine-grained turbulence by a prime ($'$), and x_i are the coordinates with x the horizontal, z the vertical and y the spanwise directions. The full Navier–Stokes equations are then split into a coherent part and a random fine-grained turbulence part by the substitution

$$u_i = U_i + u'_i, \quad p = P + p';$$

this resembles Reynolds splitting, except that the average to be taken is now the conditional average. The above formulation identifies a total mean flow, that is, the mean flow is now taken to be the sum of the usual (Reynolds averaged) mean velocity and the large-scale disturbance velocity. Thus the u'_i are random departures from the (total) mean flow and are necessarily uncorrelated, on the average, from the organized motion (Hussain & Reynolds 1970). This is entirely consistent with the original ideas of Reynolds (1895) in splitting the flow into slowly varying mean and random fluctuating parts. For an incompressible fluid we have for the dynamical variables U_i and P

$$\frac{\partial U_i}{\partial x_i} = 0, \tag{2.1}$$

$$\frac{\partial U_i}{\partial t} + \frac{\partial U_i U_j}{\partial x_j} = -\frac{\partial P}{\partial x_i} - \frac{\partial \langle u'_i u'_j \rangle}{\partial x_j} - \frac{1}{Re}\frac{\partial^2 U_i}{\partial x_j \partial x_j}, \tag{2.2}$$

where Re is the Reynolds number. The coupled but unclosed equations for the conditionally averaged stresses are

$$\left(\frac{\partial}{\partial t} + U_k\frac{\partial}{\partial x_k}\right)\langle u'_i u'_j \rangle = -\underbrace{\left[\langle u'_j u'_k \rangle\frac{\partial U_i}{\partial x_k} + \langle u'_i u'_k \rangle\frac{\partial U_j}{\partial x_k}\right]}_{\text{production}} + \underbrace{\left\langle p'\left(\frac{\partial u'_i}{\partial x_j} + \frac{\partial u'_j}{\partial x_i}\right)\right\rangle}_{\text{redistribution}}$$

$$-\frac{\partial}{\partial x_k}\underbrace{\left[\langle u'_i u'_j u'_k \rangle + \langle p'(u'_i \delta_{jk} + u'_j \delta_{ik}) \rangle - \frac{1}{Re}\frac{\partial \langle u'_i u'_j \rangle}{\partial x_k}\right]}_{\text{diffusion}} - \underbrace{2\frac{1}{Re}\left\langle\frac{\partial u'_i}{\partial x_k}\frac{\partial u'_j}{\partial x_k}\right\rangle}_{\text{dissipation}}. \tag{2.3}$$

Thus, (2.1)–(2.3) are identical to the starting point for the Reynolds equations except that the stresses $\langle u'_i u'_j \rangle$ are conditionally averaged ones, made up of $\overline{u'_i u'_j} + \tilde{r}_{ij}$, where $\overline{u'_i u'_j}$ are the mean horizontally averaged stresses and $\tilde{r}_{ij}$ are the large-scale structure-induced or modulated stresses. In this computational scheme, of course, $\langle u'_i u'_j \rangle$ appear as the dependent variables for the stresses, and this necessitates a closure scheme for the conditionally averaged quantities in

equation (2.3). Again, note that $\overline{u_i' u_j'}$, $\tilde{r}_{ij}$ and the interaction mechanisms in the mean, which do not occur explicitly, are obtainable by horizontal averaging of the numerical results.

(b) Closure of conditionally averaged quantities

Some closure schemes for conditionally averaged quantities in the $\tilde{r}_{ij}$ equation have already been discussed in the approximate energy integral analyses previously reported (Liu & Merkine 1976 a; Liu & Alper 1977; Alper & Liu 1978). That discussion was limited in that it touched upon only those quantities that are present in the shape assumptions for the integral considerations, namely the pressure–velocity correlation and viscous dissipation; notably absent are the turbulent diffusion quantities since these contribute to no net energy transfer. The main point, however, is that the shape functions $\tilde{u}_i$, or more precisely $\partial \tilde{u}_i / \partial x_j$, and $\tilde{r}_{ij}$ are obtained from approximated conservation equations. Though approximate, the energy cascade from the large-scale structure to the fine-grained turbulence, $\tilde{r}_{ij}(\partial \tilde{u}_i / \partial x_j + \partial \tilde{u}_j / \partial x_i)$, is obtained from conservation principles. In a closure scheme for equations (2.1)–(2.3), which must necessarily be more elaborate than that in the integral energy considerations (Liu & Merkine 1976 a; Liu & Alper 1977; Alper & Liu 1978), the simple but important idea of allowing the energy cascade process to follow from conservation principles should be preserved. To this end, the Launder *et al.* (1975) closure scheme is here directly extended to the conditionally averaged quantities on the right side of equation (2.3).

The philosophical ideas and pragmatic purposes of applying closure procedures to the mean quantities which have appeared in the literature on turbulence (see, for instance, Bradshaw 1972) are somewhat different from ours in that previous work has aimed at obtaining accurate computational results which can predict those mean quantities for which measurements are available. In such computational results and experiments the entire spectrum of fluctuations, including any possible large-scale coherent structures, is considered as 'turbulence.' Attempts at using the same set of 'universal' constants in predicting mean quantities in a variety of flow situations are not necessarily successful; on the other hand, different 'universal' constants might be more suitable for different flow configurations. It may well be that the fact that such constants are not necessarily universal is entirely attributable to the different instability mechanisms which give rise to the coherent structures. For instance, the mechanisms which sustain turbulent Taylor vorticities (Pai 1939, 1943; MacPhail 1941) and which account for the development and decay of the coherent structure observed by Brown & Roshko (1974) in an inflexional mean shear flow are quite different if one makes use of the wealth of physical ideas from hydrodynamic stability (Lin 1955; Stuart 1963, 1965). The fine-grained turbulence might be 'universal' but the disparately large-scale coherent structures are not. The present work, like the preceding works (Liu & Merkine 1976 a; Liu & Alper 1977; Alper & Liu 1978) which consider the large-scale structure explicitly, is directed towards obtaining a *physical understanding* of the interaction mechanisms between the disparate scales of motion rather than striving for numerical accuracy in the absence of more quantitative observations of the corresponding processes. In this situation it is difficult to assess the validity of the turbulence models used for the conditionally averaged stresses. On the other hand, the types of averaging process to be used is a matter of appropriateness for the particular physical problem of interest (see, for instance, Monin & Yaglom 1971). The conditional averaging here does separate the randomly fluctuating flow quantity from the 'slowly varying' mean flow quantity and the conservation equations for the large-scale mass and momentum and transport equations for the conditionally averaged stresses do indeed resemble

those obtained by Reynolds (1895). Thus, the use of arguments for the closure of appropriately averaged stresses of the *random* fluctuations, such as those of Launder *et al.* (1975), would be more valid here than originally anticipated. This refers to the functional forms of the closure model rather than the proportionality constants. That this may indeed be the case comes from the results of the calculations. Throughout the temporal development of the flow, the Reynolds-mean stresses, obtained from the computed conditionally averaged stresses via horizontal averaging, were monitored. The spatial variation of the Reynolds-mean stresses were consistent with the asymmetric distribution of the Reynolds-mean velocity profile. Finally, a closure framework, such as a direct extension of that of Launder *et al.* (1975) to the respective conditionally averaged quantities, will involve the simultaneous solution of the large-structure dynamics and the conditionally-averaged stresses (2.1)–(2.3) and will provide the 'proper' local energy transfer mechanisms between the various scales of motion. This is in contrast to those closure procedures that make gradient-diffusion assumptions about the stresses themselves, thereby regulating the direction of the energy transfer mechanisms at the outset.

We refer to Launder *et al.* (1975) for discussion of the closure arguments and for further references to the literature. Here, we shall make the direct extension of closure assumptions from the mean Reynolds stress transport equations to conditionally averaged stress transport equations. The closed conditionally averaged stress equation can then be written as

$$\left[\frac{\partial}{\partial t} + U_k \frac{\partial}{\partial x_k}\right]\langle u_i' u_j'\rangle = -\left[\langle u_j' u_k'\rangle \frac{\partial U_i}{\partial x_k} + \langle u_i' u_k'\rangle \frac{\partial U_j}{\partial x_k}\right] - c_1 \frac{\langle \epsilon \rangle}{\langle k \rangle}\left[\langle u_i' u_j'\rangle - \tfrac{2}{3}\delta_{ij}\langle k \rangle\right]$$

$$-\gamma[\langle P_{ij}\rangle - \tfrac{1}{3}\delta_{ij}\langle P_{kk}\rangle] + c_s' \frac{\partial}{\partial x_k}\left[\frac{\langle k \rangle}{\langle \epsilon \rangle}\langle u_k' u_l'\rangle \frac{\partial \langle u_i' u_j'\rangle}{\partial x_l}\right] - \tfrac{2}{3}\delta_{ij}\langle \epsilon \rangle. \qquad (2.4)$$

The first term on the right of equation (2.4) represents production. The second and third terms on the right come from the pressure–velocity correlation assumption. The second term follows directly from Rotta (1951) by using Chou's (1945) Poisson equation argument; $\langle \epsilon \rangle$ here is the conditionally averaged (dimensionless) viscous dissipation rate, $\langle k \rangle = \tfrac{1}{2}\langle u_i'^2\rangle$ is the conditionally averaged fine-grained turbulence kinetic energy and c_1 is taken to be a constant ($c_1 = 1.5$). The third term on the right, which gives rise to a tendency towards isotropizing the local turbulence production, follows from a simplified version (model 2) of Launder *et al.* (1975) where γ is taken as constant ($\gamma = 0.6$), and $\langle P_{ij}\rangle$ is the conditionally averaged fine-grained turbulence kinetic energy production rate:

$$\langle P_{ij}\rangle = -\langle u_i' u_k'\rangle \frac{\partial U_j}{\partial x_k} - \langle u_j' u_k'\rangle \frac{\partial U_i}{\partial x_k},$$

that is, the production of $\langle k \rangle$ from the local large-scale coherent structure rates of strain $\partial U_i/\partial x_j$. Hence, the effects of local rapid distortion due to the large-scale structure are appropriately accounted for by the third term in (2.4). Among the diffusion terms in (2.3) only the triple correlation terms are retained and their closure follows from direct extension of the simple gradient diffusion hypothesis of Daly & Harlow (1970) to the corresponding conditionally averaged quantity here and is represented by the fourth term in (2.4), where c_s' is taken as constant ($c_s' = 0.25$). The viscous decay terms in (2.3) are taken to be isotropic. That is, they are taken to contribute to the rate of dissipation of the fine-grained turbulence kinetic energy but not to the off-diagonal stresses. Hence, the last term of (2.4) is

$$\frac{2}{Re}\left\langle \frac{\partial u_i'}{\partial x_l} \frac{\partial u_j'}{\partial x_l}\right\rangle = \tfrac{2}{3}\delta_{ij}\langle \epsilon \rangle. \qquad (2.5)$$

The use of (2.5) here, which refers to the fine-grained turbulence which is most likely to be isotropic, is more logically viable than for the Reynolds mean that includes the large-scale coherent structure which could contribute to much of the anisotropy. The exact equation for $\langle \epsilon \rangle$ is then modelled via Hanjalić & Launder (1972):

$$\left(\frac{\partial}{\partial t} + U_i \frac{\partial}{\partial x_i}\right) \langle \epsilon \rangle = c_\epsilon \frac{\partial}{\partial x_k} \left(\frac{\langle k \rangle}{\langle \epsilon \rangle} \langle u_k' u_l' \rangle \frac{\partial \langle \epsilon \rangle}{\partial x_l}\right) - c_{\epsilon 1} \frac{\langle \epsilon \rangle}{\langle k \rangle} \langle u_i' u_k' \rangle \frac{\partial U_i}{\partial x_k} - c_{\epsilon 2} \frac{\langle \epsilon \rangle}{\langle k \rangle} \langle \epsilon \rangle, \tag{2.6}$$

The first term on the right depicts the diffusion of $\langle \epsilon \rangle$, and the second and third give the effects of stretching and viscous decay on $\langle \epsilon \rangle$; c_ϵ, $c_{\epsilon 1}$ and $c_{\epsilon 2}$ are taken as constants ($c_\epsilon = 0.15$, $c_{\epsilon 1} = 1.44$, $c_{\epsilon 2} = 1.9$).

We have eleven equations for eleven unknowns, in general: four dynamical variables of the large-scale structure U_i, P; six conditionally averaged fine-grained turbulence stresses $\langle u_i' u_j' \rangle$ and the conditionally averaged viscous dissipation rate $\langle \epsilon \rangle$.

3. The numerical calculation procedure

We shall apply the framework discussed in detail above (see also Liu & Alper 1977) to consider the horizontally periodic and temporally amplifying two-dimensional large-scale structure in the mixing region of oppositely directed streams, a problem considered approximately by Liu & Merkine (1976a). The vorticity axis of the large-scale structure is in the spanwise, y-direction and the velocities U, W are in the x- and z-directions, respectively. The spanwise velocity V is zero, and so are all spanwise gradients of the conditionally averaged quantities. In this case the equations and unknowns reduce to eight for U, W, P, $\langle u'w' \rangle$, $\langle u'^2 \rangle$, $\langle w'^2 \rangle$, $\langle v'^2 \rangle$ and $\langle \epsilon \rangle$, in the case of the simple gradient diffusion model used. The fine-grained turbulence is, of course, three-dimensional, but $\partial \langle u_i' u_j' \rangle / \partial y = 0$, as already noted. It is advantageous to re-formulate the problem in terms of the vorticity and stream function of the large-scale structure. Such a formulation allows the elimination of the pressure as a dependent variable. Upon introducing the stream function

$$U = \frac{\partial \Psi}{\partial z}, \quad W = -\frac{\partial \Psi}{\partial x}, \tag{3.1}$$

the continuity equation (2.1) is automatically satisfied. The vorticity is then related to the stream function by definition:

$$\Omega = -\nabla^2 \Psi, \tag{3.2}$$

where $\nabla^2 = \partial^2/\partial x^2 + \partial^2/\partial z^2$ is the Laplacian in the (x, z) plane. Thus, with (3.1) and (3.2), the continuity and momentum equations (2.1) and (2.2) are replaced by the vorticity equation in terms of the stream function

$$\nabla^2 \Psi_t + \Psi_z \nabla^2 \Psi_x - \Psi_x \nabla^2 \Psi_z = \langle u'w' \rangle_{xx} - \langle u'w' \rangle_{zz} + (\langle w'^2 \rangle - \langle u'^2 \rangle)_{xz}, \tag{3.3}$$

where the subscripts indicate the appropriate partial differentiation. Thus the number of dynamical equations for the large-scale structure is reduced from three to one if Ψ and the definition of Ω are used.

(a) Boundary conditions

The boundary conditions of the problem require that the large-scale structure quantities and the conditionally averaged turbulent stresses and viscous dissipation rate vanish as $|z| \to \infty$, with the stream function being a linear function of z so that $\Psi_z \to \bar{U} = 1$ as $|z| \to \infty$. Computationally,

the vertical field is taken to be sufficiently large that the above boundary conditions are approximately satisfied. In the horizontal x-direction the field chosen is one large-scale structure wavelength (to be fixed by the initial condition) and the boundary conditions there require that the large-scale structure quantities as well as the conditionally averaged turbulent correlations be periodic.

(b) Initial conditions

Initially, at $t = t_0$, we envision that there exists a mean turbulent mixing layer consisting of oppositely directed, horizontally homogeneous streams. Such a mean flow coexists with a set of compatible mean turbulent stresses and dissipation rate. At $t = t_0$ a large-scale structure is imposed so that the initial condition for (3.3) in terms of Ψ becomes

$$\Psi(x, z; t_0) = \overline{\Psi}(z; t_0) + \tilde{\psi}(x, z; t_0). \tag{3.4}$$

The initial conditions for the stresses of (2.4) and for the dissipation rate of (2.6) become

$$\langle u_i' u_j' \rangle(x, z; t_0) = \overline{u_i' u_j'}(z; t_0) + \tilde{r}_{ij}(x, z; t_0), \tag{3.5}$$

$$\langle \epsilon \rangle(x, z; t_0) = \bar{\epsilon}(z; t_0) + \tilde{\epsilon}(x, z; t_0), \tag{3.6}$$

respectively. The mean flow is horizontally homogeneous so that all x-derivatives of $\overline{\Psi}$, $\overline{u_i' u_j'}$ and $\bar{\epsilon}$ vanish. The imposed coherent quantities $\tilde{\psi}$, $\tilde{r}_{ij}$ and $\tilde{\epsilon}$ are to be hydrodynamically possible disturbances that are consistent with the prevailing mean flow, rather than arbitrarily imposed functions. They may be obtained, for instance, from a linearized theory which nevertheless couples the calculation for $\tilde{\psi}$, $\tilde{r}_{ij}$ and $\tilde{\epsilon}$. Following arguments of Liu & Merkine (1976a), it would appear that the simple description of $\tilde{\psi}$ in terms of the Rayleigh equation suffices, with $\tilde{r}_{ij}$ and $\tilde{\epsilon}$ set equal to zero in the initial disturbance level. These initialization procedures will be discussed in §§ 4 and 5.

The subsequent numerical method used in the computations will be a finite-difference technique. The explicit finite-difference scheme to be used is the simple forward time centre space (f.t.c.s.) scheme. Although restrictive in time-step size, it requires a minimum of programming development for the particular geometry at hand. Throughout the system of equations, the formal accuracy of the discretization is $O(\Delta t, \Delta x^2, \Delta z^2)$. In addition, computational experiments were performed to insure adequate resolution and accurate results (consistent with the formal accuracy of the finite-difference scheme) in regions of high shear. Of course, without experimental results only relative comparisons such as these can be performed to check the validity of the computational results. The stream function of (3.3) (as well as the vorticity of (3.2) and the shear stress of (2.4)) is defined at the corners of a computational cell and all other variables are defined at the centre of each cell. The grid spacings are equal in the x and z directions with 21 grid points in the x direction and a maximum of 35 grid points in the z direction. The vertical range varied by a factor of about two to allow for the growth of the shear layer thickness. Before the computation, however, the set of self-consistent initial conditions (3.4)–(3.6) must be obtained. This is discussed in §§ 4 and 5 below.

4. Initialization of the mean velocity, Reynolds stresses and dissipation rate

It is important to discuss the more quantitative aspects of this 'initialization' process which leads to a set of consistent initial data to start the integration of (3.3). The proper initialization will enable us to study the subsequent nonlinear interaction processes as a result of the non-equilibrium interactions between the large-scale structure and the fine-grained turbulence without the complicating influence of the adjustment between the mean flow and the mis-matched, incompatible mean turbulent stresses and dissipation rate. This is not to say that the choice of initialization here is the correct choice for the modelling of a real turbulent flow; indeed, the correct choice of initial conditions in the modelling of turbulent flows is probably of central importance to accurately match modelled and experimental results. However, in such a controlled experiment where the study of the interaction dynamics is the issue, the proper initialization is the one chosen. To achieve a set of self-consistent mean flow quantities devoid of large-scale structure, the mean equations are obtained from the previously discussed equations for the total quantities by setting the contributions from the large-scale structure equal to zero. The continuity equation (2.1) leads to $\bar{U} = \bar{U}(z, t)$ for the mean velocity. From (2.4) it follows that $\overline{v'^2} = \overline{w'^2}$ since they have no direct production mechanisms.† The boundary conditions for $\bar{U}$ are that as $z \to \pm \infty$, $\bar{U} \to \pm 1$ and that the stresses and dissipation rate vanish. The starting values for the time integration are a hyperbolic tangent profile for $\bar{U}$ and a set of functions for the stresses similar to those used by Liu & Merkine (1976a) in their shape assumption. The choice of these functions is guided by the results in the homogeneous shear problem (Lumley 1970) for the ratios among the normal and shear stresses and the observational results of Wygnanski & Fiedler (1970) for the vertical distributions. The starting value for the viscous dissipation rate was taken to be $\bar{\epsilon} = 0.3\bar{k}\, \partial U/\partial z$, which implies a balance of dissipation and production of kinetic energy for most of the shear layer. On a point by point basis, the vertical distributions of these starting values are not necessarily self-consistent. With these starting values, numerical integration of the system of equations for the temporal development of the mean turbulent shear layer was carried out by using the f.t.c.s. scheme discussed in §3. Calculations proceeded until the mean velocity and the stresses evolved to a consistent self-preserving form. Following Townsend (1976), the instantaneous mean shear layer thickness was defined as the variance of the distribution of velocity gradient,

$$\delta(t) = \left[\int z^2 \partial \bar{U}/\partial z\, \mathrm{d}z \Big/ \int \partial \bar{U}/\partial z\, \mathrm{d}z \right]^{\frac{1}{2}}, \tag{4.1}$$

where the limits of integration expanded continuously with time so that the domain of integration far from the centre line included the region where $\partial \bar{U}/\partial z = 0$.

In this two dimensional mixing layer, self-preserving development is assumed when numerically $\mathrm{d}\delta/\mathrm{d}t$ is very nearly constant. It must be noted that in the development of a real turbulent flow such self-preserving development may only be achieved as some asymptotic condition which may or may not be actually realized within the confines of the experimental apparatus. As we have discussed, the starting values for the initialization computation for the mean velocity, Reynolds stresses and viscous dissipation rate are analytically represented for convenience and are in self-preservation form. However, these starting profiles, which are not necessarily self-

† This is not true, however, for $\langle u'^2 \rangle$ and $\langle w'^2 \rangle$ because of their production from the large-scale structure.

consistent, are subsequently made self-consistant by the end of the initialization computation. The self-consistent set of self-preservation profiles obtained are indeed the end result and primary purpose of the initialization computations here. These differ quantitatively (but not qualitatively) from the starting profiles and are not analytically representable in a simple manner.

Self-preservation, of course, does not necessarily imply that the flow is in equilibrium in that the production balances the rate of viscous dissipation across the entire shear layer. It implies here only that the profiles of the mean flow, stresses and viscous dissipation rate are self similar in their development. In fact, there is a relatively small but residual imbalance between overall fine-grained turbulence energy production over the viscous dissipation so that this provides the initial turbulence energy increase in the subsequent large-scale interaction problem.

The self-preserving mean velocity profile obtained here will furnish $\overline{\Psi}(z; t_0)$, the first part of the initial condition (3.4). The first part of the initial conditions for the stresses and dissipation rate (3.5) and (3.6) is thus also obtained. We now go on to determine the initial large-scale structure distribution which must be consistent with the prevailing mean shear flow just obtained.
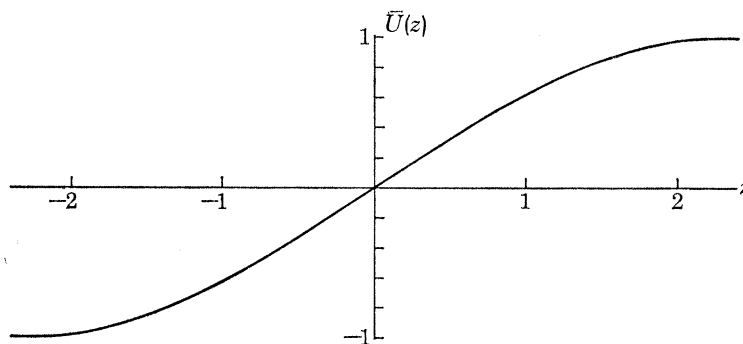

FIGURE 1. The self-preserving initial mean velocity profile.

5. INITIALIZATION OF THE LARGE-SCALE STRUCTURE

The initial large-scale disturbance will now be determined by using the self-preserving form of the mean velocity profile (figure 1) just obtained, where $\delta(t) \approx 3.6$. (Note, the vertical co-ordinate z in figure 1 is now rescaled by $\delta = 3.6$, but, for notational convenience, the coordinate designations x, z will be retained although, as will be noted, further rescaling may be necessary.) As pointed out earlier, $\tilde{\psi}(x, z; t_0)$ can be determined from a linearized theory which couples $\tilde{\psi}$, $\tilde{r}_{ij}$ and $\tilde{\varepsilon}$ according to the framework discussed in §2. However, the instability which arises is most likely to be a dynamical one associated with the inflexional mean profile. In this case, Liu & Merkine (1976a) gave arguments that it is sufficient to determine $\tilde{\psi}$ from 'inviscid' considerations, that is, from the Rayleigh equation as a first approximation. Thus we represent $\tilde{\psi}$ by

$$\tilde{\psi}(x, z; t_0) = A(t_0)\, \phi(z; \alpha) \exp(i\alpha x) + \text{c.c.}, \tag{5.1}$$

where the eigenfunction $\phi(z; \alpha)$ satisfies the Rayleigh equation

$$(\overline{U} - c)(\phi'' - \alpha^2 \phi) - \phi \overline{U}'' = 0. \tag{5.2}$$

Here the primes indicate differentiation with respect to the normalized z, α is the real wave number normalized by δ_0 and c is the complex phase velocity (which is merely ic_i, the imaginary phase velocity, since the real phase velocity c_r is zero in the present problem). The outer boundary

condition for ϕ is just $\phi' + \alpha\phi \to 0$; that is, ϕ and ϕ' decay exponentially far from the centre of the shear layer. The numerical solution procedures for (5.2) are well known (see, for instance, Michalke 1964) for any given mean velocity profile $\bar{U}(z; t_0)$. The results of the eigenvalue calculation for the self-preserving mean velocity profile (see figure 1) obtained in §4 are given in figure 2, which shows the eigenvalue c_i and amplification rate αc_i as functions of the wave number α. The most amplified disturbance occurs at about $\alpha \approx 0.275$ with $c_i \approx 0.4716$ and $\alpha c_i \approx 0.1297$. The most amplified disturbance will be used in (5.1) and in (3.4) as the initial condition. Our mean velocity profile differs from the tanh z profile and therefore the resulting eigenvalues are correspondingly different from those for that profile.
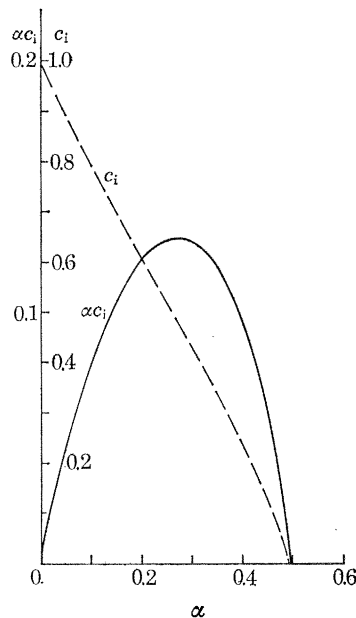
FIGURE 2. Hydrodynamic stability characteristics of the large-scale structure consistent with initial mean velocity profile. The most amplified mode is used as initial condition. ——, αc_i (growth rate); – – –, c_i (complex phase speed).

Since the eigenfunction is linear, it is determined up to an arbitrary constant denoted by $A(t_0)$ in (5.1). In order to render this arbitrary constant unique and physically meaningful, the eigenfunctions themselves are normalized so that

$$\int_{-\infty}^{\infty} (|\phi'|^2 + \alpha^2|\phi|^2)\, dz = 1.$$

This then fixes the physical meaning of $|A|^2$ as the energy density, the total large-scale structure kinetic energy per unit δ_0 contained in an area bounded by the shear layer thickness in the vertical and by one wavelength $2\pi/\alpha$ in the horizontal (see, for instance, Liu & Merkine 1976a). Thus in specifying $A(t_0)$ in the initial condition (3.4), one specifies the initial energy level of the imposed large-scale disturbance.

Following the arguments of Liu & Merkine (1976a), one can then calculate $\tilde{r}_{ij}(x, z; t_0)$ and $\tilde{\epsilon}(x, z; t_0)$ from the linear theory using the eigenfunction $\phi(x, z; t_0)$ just obtained, and these then furnish the remaining initial conditions in (3.5) and (3.6). For simplicity we set $\tilde{r}_{ij}(x, z; t_0) = 0$ and $\tilde{\epsilon}(x, z; t_0) = 0$. However, it can be argued that since the large-scale structure is considered

to be *suddenly* imposed and the modulation of the turbulence by this structure would take a finite time to accomplish, both the modulated stresses $\tilde{r}_{ij}(x, z; t_0)$ and dissipation rate $\tilde{\epsilon}(x, z; t_0)$ would remain in their frozen state of zero as far as the initial condition is concerned.

6. Numerical results

The physical quantities that characterize both the large-scale structure and the fine-grained turbulence are their respective kinetic energy integrals,

$$E_1 \equiv \delta |A|^2 = \frac{1}{2} \int_{-\infty}^{\infty} \overline{(\tilde{u}^2 + \tilde{w}^2)} \, dz, \qquad (6.1)$$

$$E_t \equiv \delta E = \frac{1}{2} \int_{-\infty}^{\infty} \overline{(u'^2 + v'^2 + w'^2)} \, dz, \qquad (6.2)$$

(the notation used is that in Liu & Merkine 1976 *a*). The physical lengths here are normalized by the initial shear layer thickness, where δ is the local shear layer thickness. Hence $|A|^2, E$ are the corresponding energy densities (though these are not explictly used here) while E_1, E_t are respectively the large-scale structure and turbulence kinetic energy contained in a 'box' of unit width bounded horizontally by one wavelength of the large-scale structure and vertically by the extent of the shear layer. The numerical integration started with an initial fine-grained turbulence field given by the initialization process described in § 4. That yielded an initial turbulence energy level of $E_{t0} = E_0 = 1.20 \times 10^{-2}$. The initial large-scale structure energy level was taken as $E_{10} = |A|_0^2 = 10^{-4}$, which corresponds to initial root-mean-square velocity disturbance of a small percentage of the free stream velocity. The initial mode shape was taken to be that of the most-amplified mode, as discussed in § 5. In the subsequent parts of this section we will discuss the mechanisms for the evolution of E_1 and E_t. First, however, it is appropriate to discuss the direct results of the numerical calculations in terms of the conditionally averaged streamline and vorticity patterns.

(a) Development of conditionally averaged stream function and vorticity

The stream function $\Psi(x, z; t)$, which consists of the sum of the mean flow $\overline{\Psi}(z; t)$ and the large-scale structure $\tilde{\psi}(x, z; t)$, is shown in figures 3 (*a*)–(*g*) for the times indicated. In the final results presented, all the coordinates are normalized by the wavelength of the initial disturbance, and the timescale should now be understood to be scaled by the wavelength of the initial disturbance and the free stream velocity. The vertical extent of the structure, as indicated by the conditionally averaged streamlines, spreads rapidly and reaches a plateau at about $t \approx 1.5$–2, after which it begins to subside. The stream function contours are the cats'-eye patterns familiar in the corresponding physical problem in laminar flow. No qualitative deviations from the cats'-eye pattern occurred during the development of the flow. One can say, in general, that as far as free shear flows are concerned, the nonlinear instability patterns found in laminar inflexional flows are also possible in turbulent shear flows. However, the nonlinear mechanisms of development are quite different from those in the much simpler corresponding laminar flows.

The conditionally averaged vorticity contours are shown in figures 4 (*a*)–(*h*). Again, the vorticity $\Omega(x, z; t)$ consists of the sum of the mean vorticity $\overline{\Omega}(z; t)$ and the large-scale structure vorticity $\tilde{\omega}(x, z; t)$. The initial large-scale structure corresponding to the most-amplified mode has a double concentration of vorticity (figure 4 (*a*)) (see figure 1 of Michalke (1965)), but
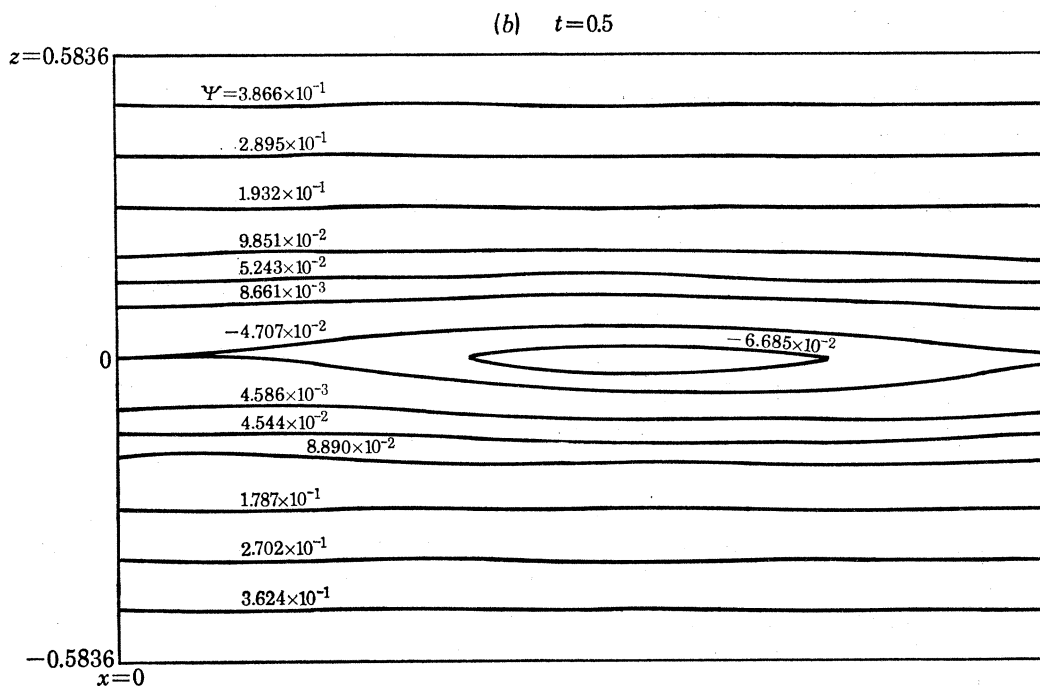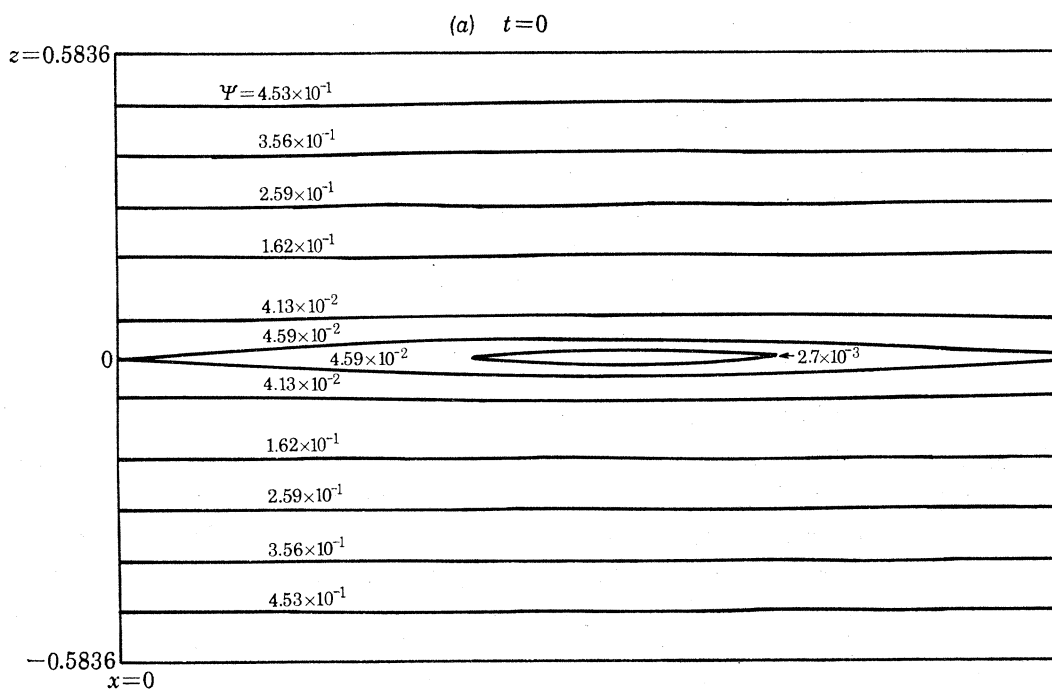
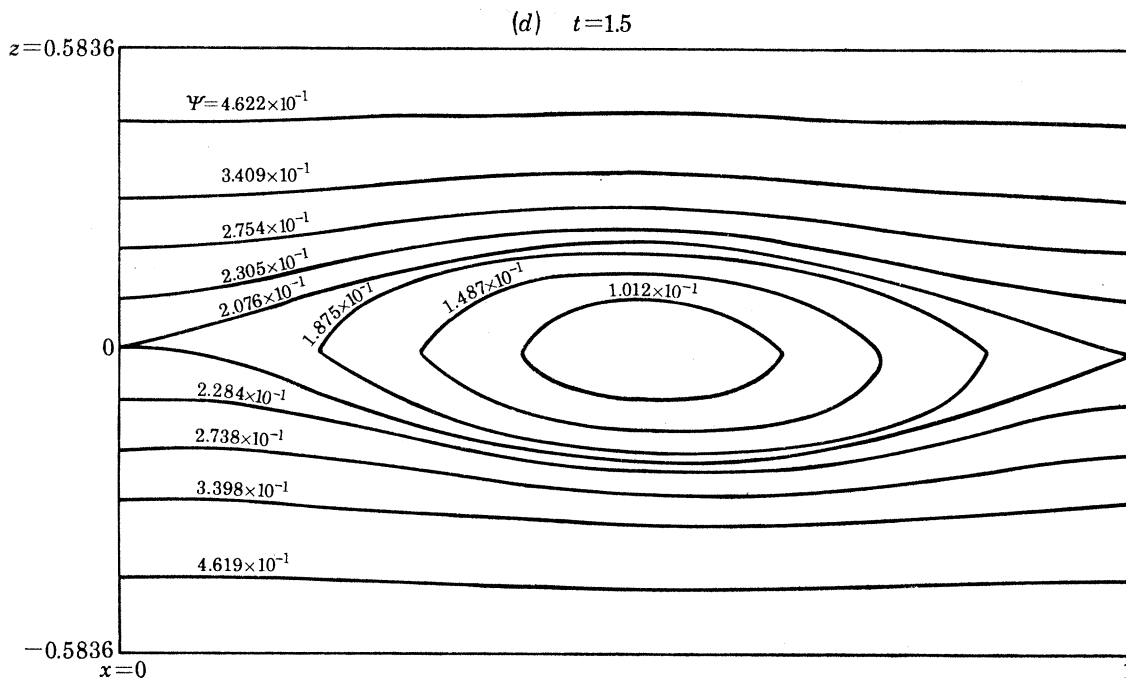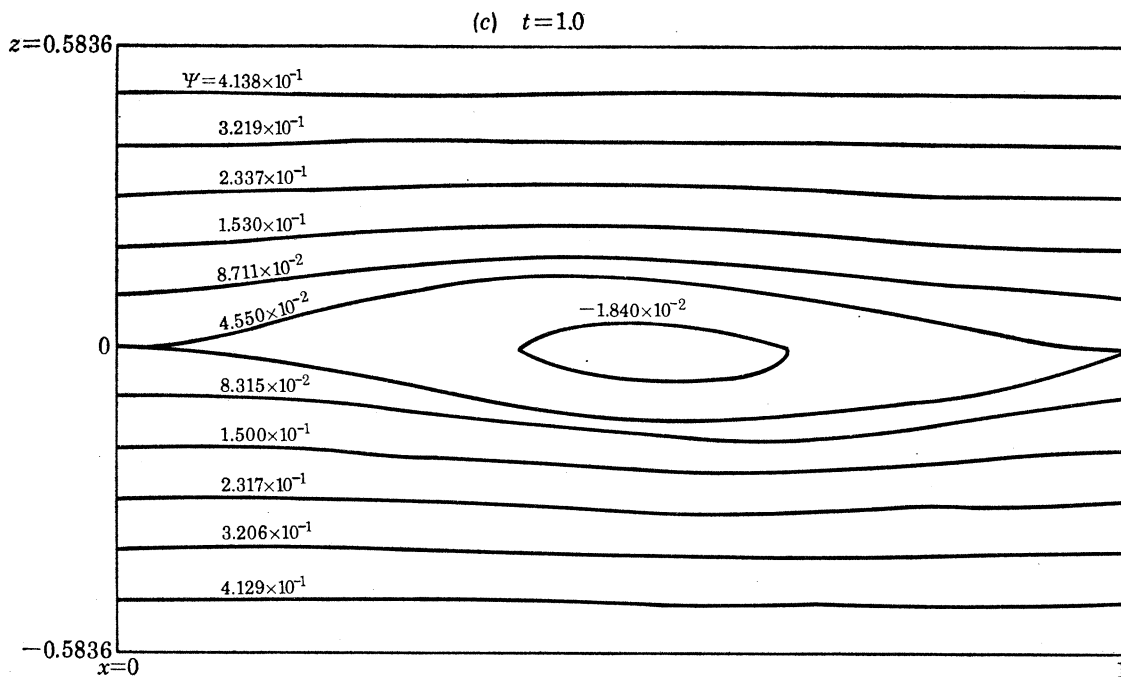FIGURE 3a AND b. For description see p. 489.
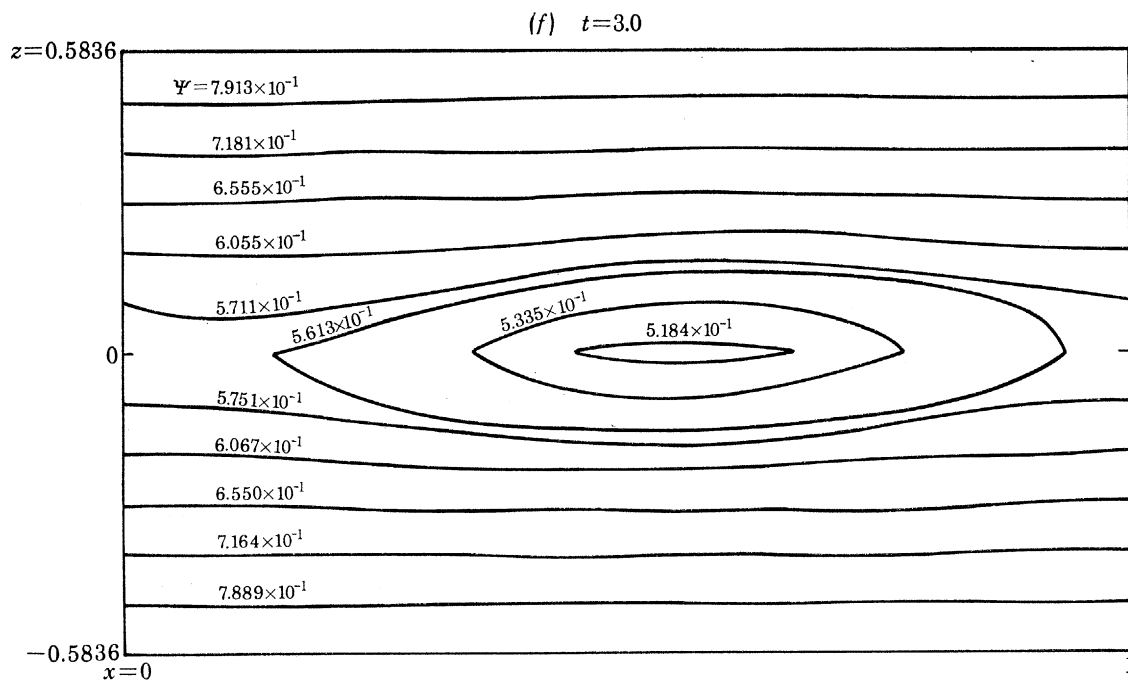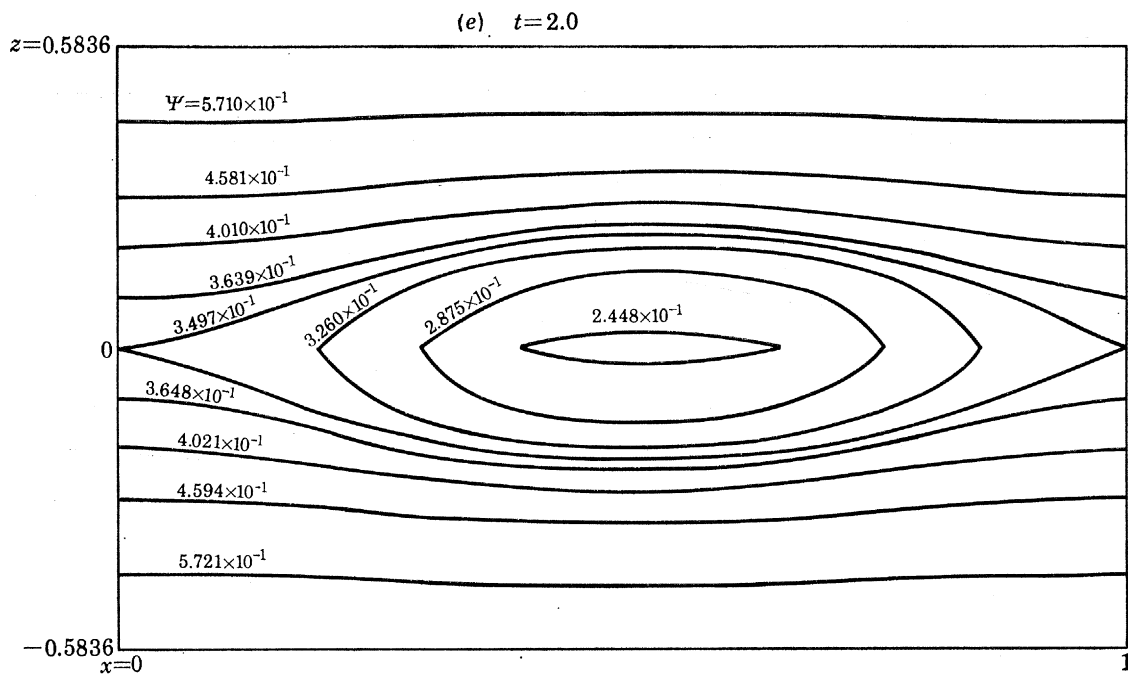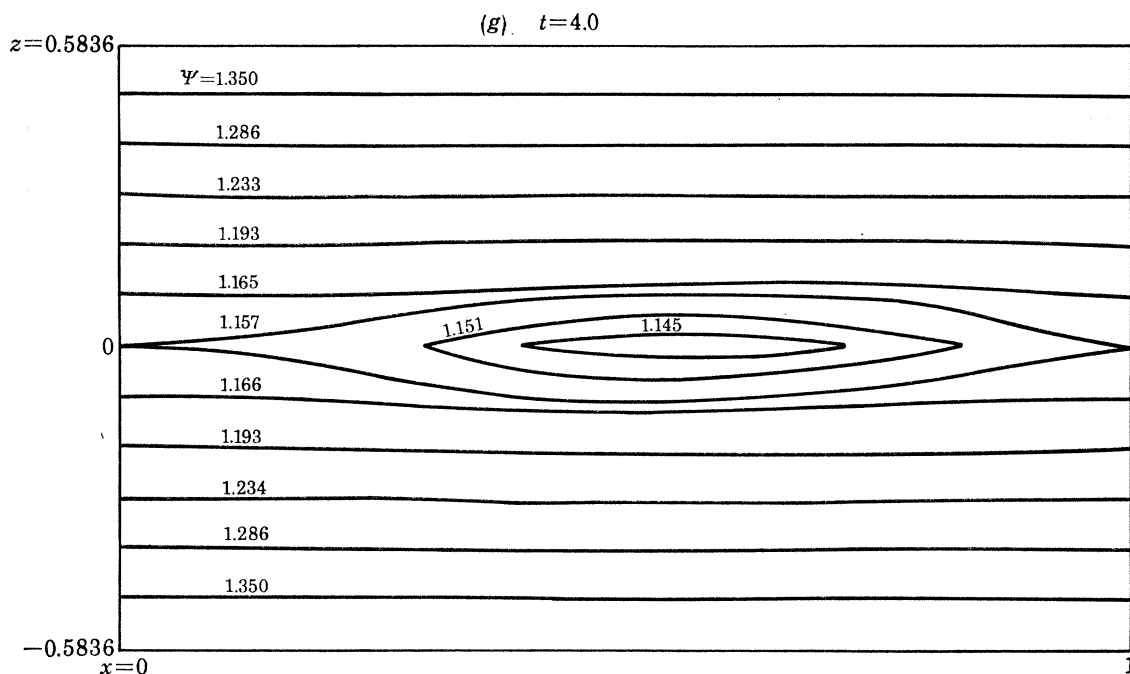
FIGURE 3c AND d. For description see p. 489.

(e) $t = 2.0$

$z = 0.5836$

$\Psi = 5.710 \times 10^{-1}$

4.581×10^{-1}

4.010×10^{-1}

3.639×10^{-1}

3.497×10^{-1}

3.260×10^{-1}

2.875×10^{-1}

2.448×10^{-1}

0

3.648×10^{-1}

4.021×10^{-1}

4.594×10^{-1}

5.721×10^{-1}

-0.5836

$x = 0$

1

(f) $t = 3.0$

$z = 0.5836$

$\Psi = 7.913 \times 10^{-1}$

7.181×10^{-1}

6.555×10^{-1}

6.055×10^{-1}

5.711×10^{-1}

5.613×10^{-1}

5.335×10^{-1}

5.184×10^{-1}

0

5.751×10^{-1}

6.067×10^{-1}

6.550×10^{-1}

7.164×10^{-1}

7.889×10^{-1}

-0.5836

$x = 0$

1

FIGURE 3e AND f. For description see opposite.

FIGURE 3. Time development of conditionally averaged stream function contours. (a) $t = 0$,
(b) $t = 0.5$, (c) $t = 1.0$, (d) $t = 1.5$, (e) $t = 2.0$, (f) $t = 3.0$, (g) $t = 4.0$.

this very quickly agglomerates into a single concentration and remains single through about $t \approx 1.0$. At about $t \approx 1.5$ a three-cell vorticity structure emerges and appears to remain in the subsequent development. However, the local intensity of the conditionally averaged vorticity appears to be progressively weakened under the action of the conditionally averaged turbulent stresses. In addition, the change of symmetry occurring in this time frame is also due to the action of the conditionally averaged stresses rather than due to any 'roll over' of the structure in the central core region. As in the conditionally averaged streamline patterns of figures $3(a)$–(g), the vertical extent of the corresponding vorticity pattern spreads rapidly until $t \approx 1.5$–2.0, after which its vertical extent also collapses somewhat.

(b) Interactions between disparate scales of motion in the mean

In order to understand physically the overall interaction processes in the problem, horizontal averages of the numerical results are taken so as to enable us to diagnose the temporal interactions, in the (horizontal) mean, between the mean motion, large-scale coherent structure and fine-grained turbulence.

The kinetic energy equations for the three components of motion can be written as (see also Liu & Merkine 1976a):

$$\mathrm{d}E_\mathrm{m}/\mathrm{d}t = -\tilde{I}_\mathrm{p} - I'_\mathrm{p}, \tag{6.3}$$

$$\mathrm{d}E_1/\mathrm{d}t = \tilde{I}_\mathrm{p} - I_{1\mathrm{t}}, \tag{6.4}$$

$$\mathrm{d}E_\mathrm{t}/\mathrm{d}t = I'_\mathrm{p} + I_{1\mathrm{t}} - \overline{\phi'}. \tag{6.5}$$

The mean flow kinetic energy defect is

$$E_\mathrm{m} = \int_{-\infty}^{0} (\bar{U}^2 - \bar{U}_{-\infty}^2)\,\mathrm{d}z + \int_{0}^{\infty} (\bar{U}^2 - \bar{U}_\infty^2)\,\mathrm{d}z, \tag{6.6}$$
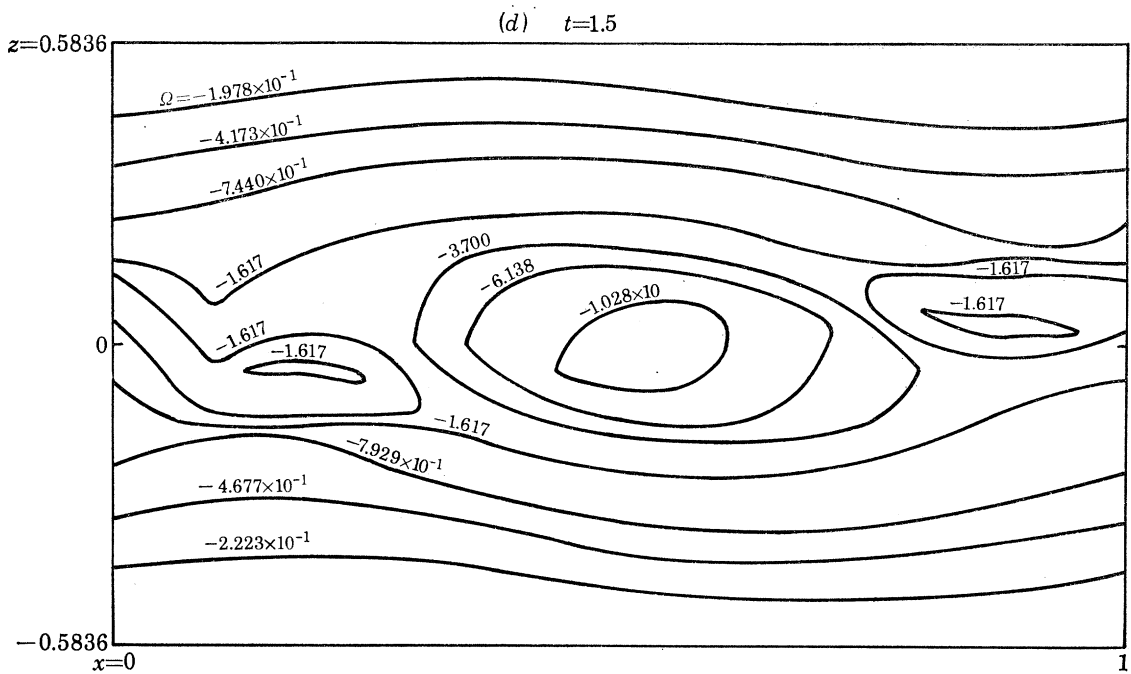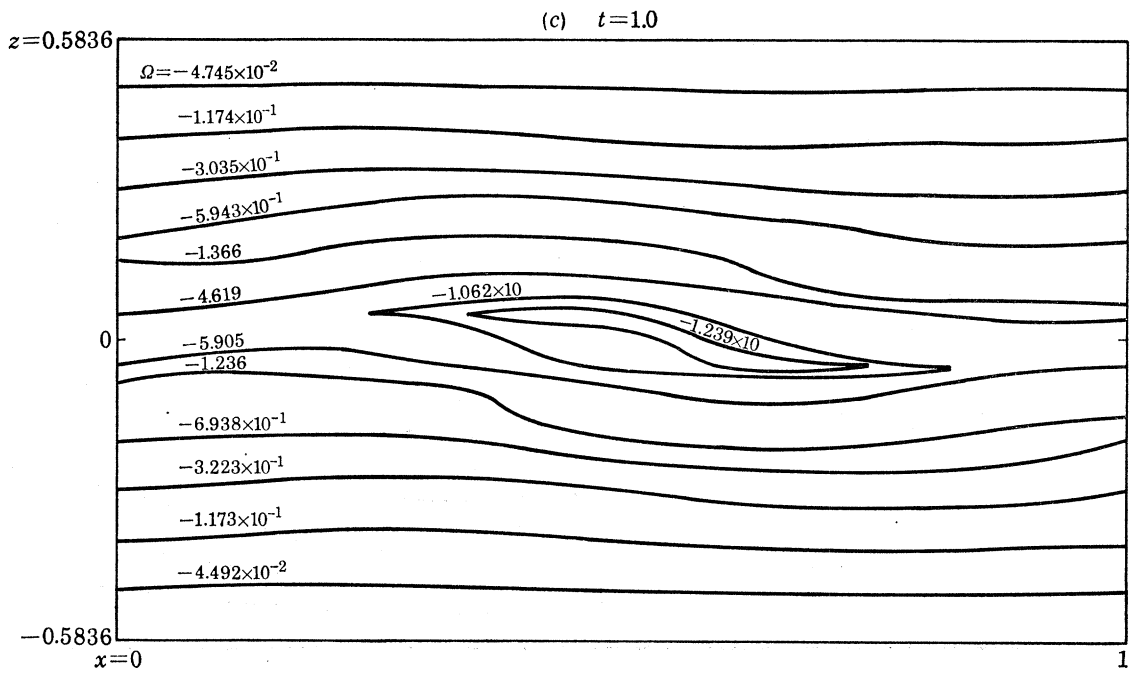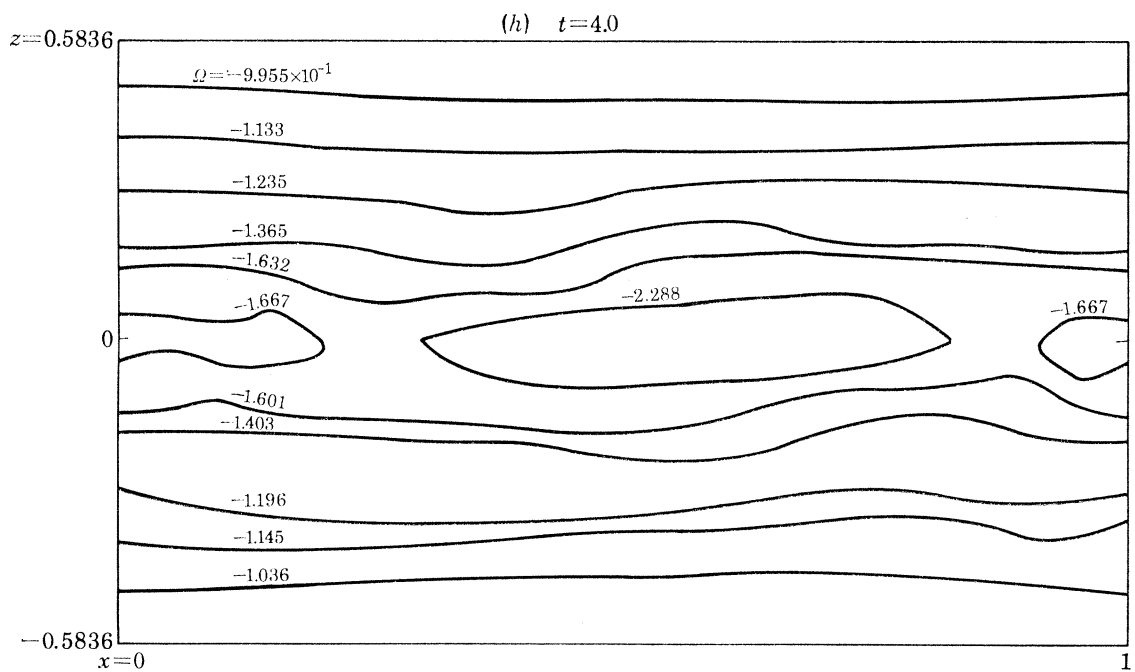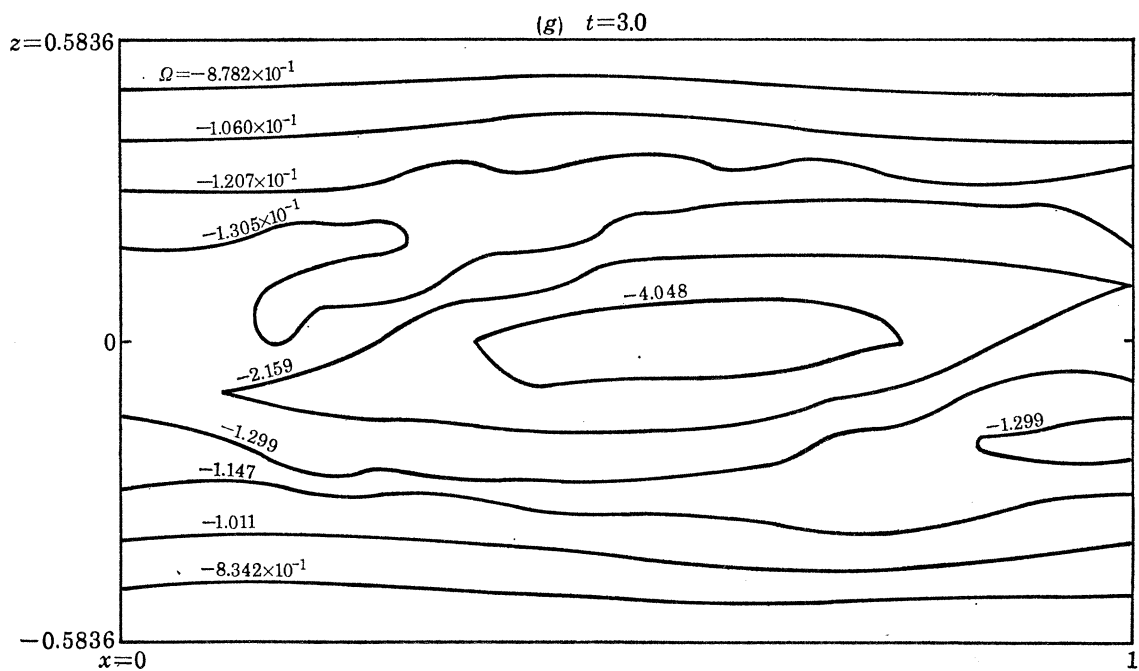
(a) $t=0$

$z=0.5836$

$\Omega=-1.290\times10$

0   -1.290×10 -1.504×10 1.504×10

-0.5836

$x=0$ 1

(b) $t=0.5$

$z=0.5836$

$\Omega=-1.458\times10^{-4}$

-3.604×10^{-3}

-4.115×10^{-2}

-2.182×10^{-1}

-8.164×10^{-1}

-2.306

-8.141

0   -9.146 -1.295×10

-9.158×10^{-1}

-2.407×10^{-1}

-4.635×10^{-2}

-6.474×10^{-3}

-1.041×10^{-4}

-0.5836

$x=0$ 1
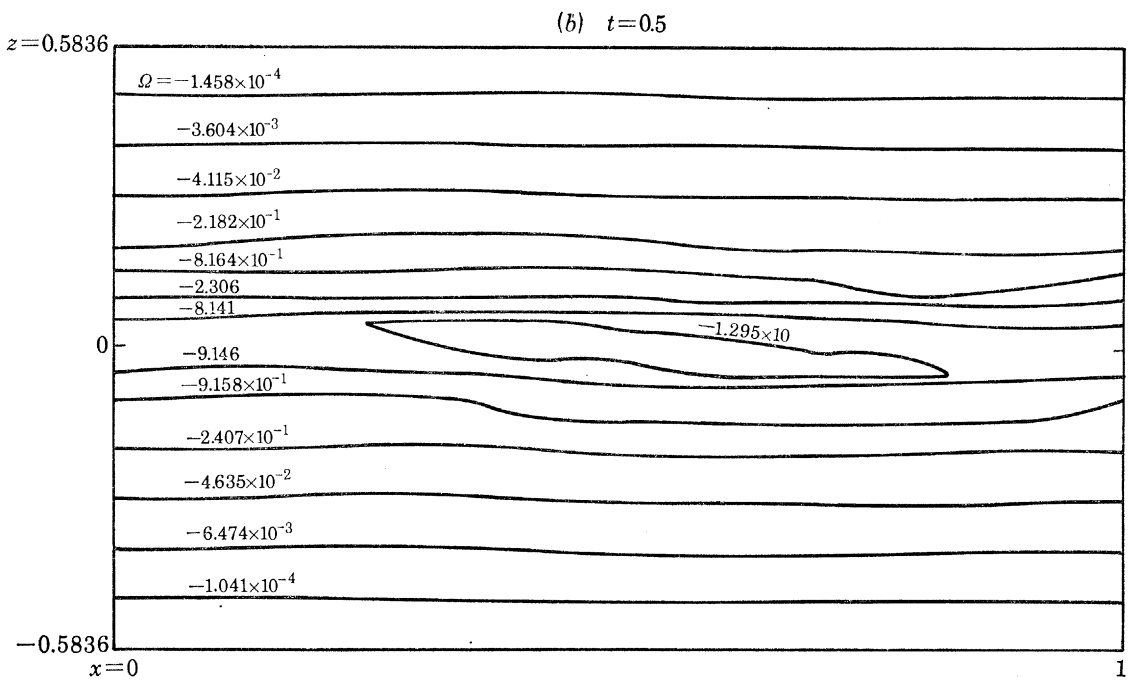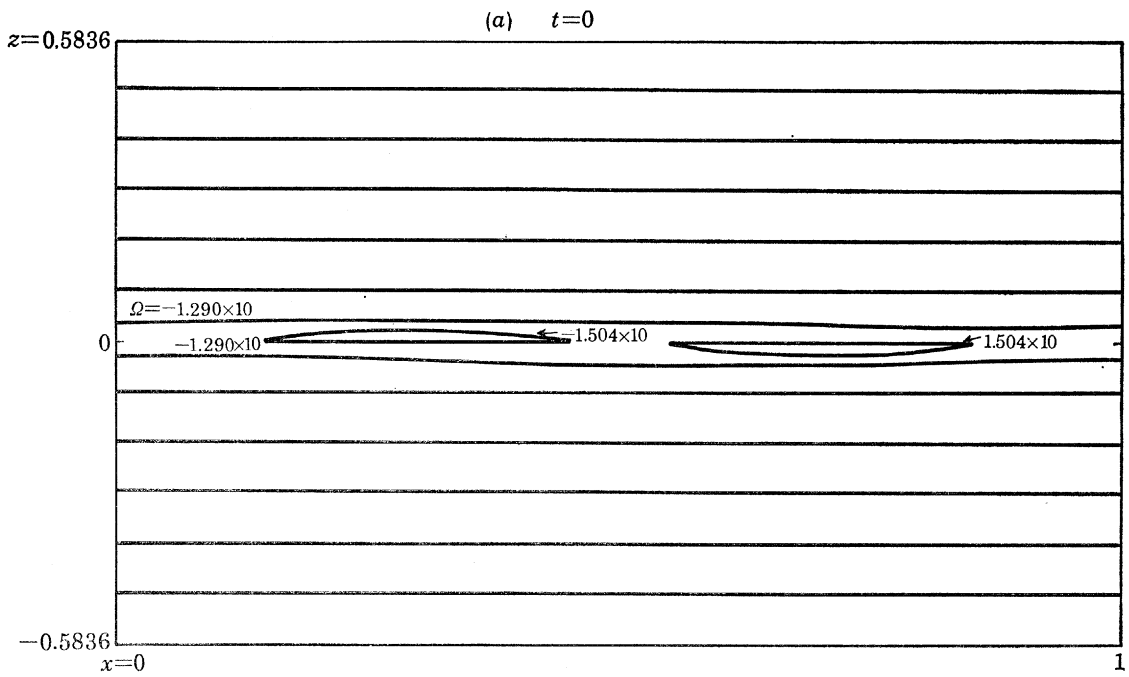
FIGURE 4 a AND b. For description see p. 493.

(c) $t=1.0$

(d) $t=1.5$

FIGURE 4c AND d. For description see p. 493.

FIGURE 4e AND f. For description see opposite.

FIGURE 4. Time development of conditionally averaged vorticity contours. (a) $t = 0$, (b) $t = 0.5$, (c) $t = 1.0$, (d) $t = 1.5$, (e) $t = 1.75$, (f) $t = 2.0$, (g) $t = 3.0$, (h) $t = 4.0$.

where $\bar{U}_{\pm\infty} = \pm 1$ are the dimensionless upper and lower streams external to the shear layer, and E_l and E_t are as defined in (6.1) and (6.2), respectively. The large-scale structure and fine-grained turbulence production integrals are

$$\tilde{I}_p = \int_{-\infty}^{\infty} -\overline{\tilde{u}\tilde{w}}\frac{\partial \bar{U}}{\partial z}dz, \tag{6.7}$$

$$I'_p = \int_{-\infty}^{\infty} -\overline{u'w'}\frac{\partial \bar{U}}{\partial z}dz. \tag{6.8}$$
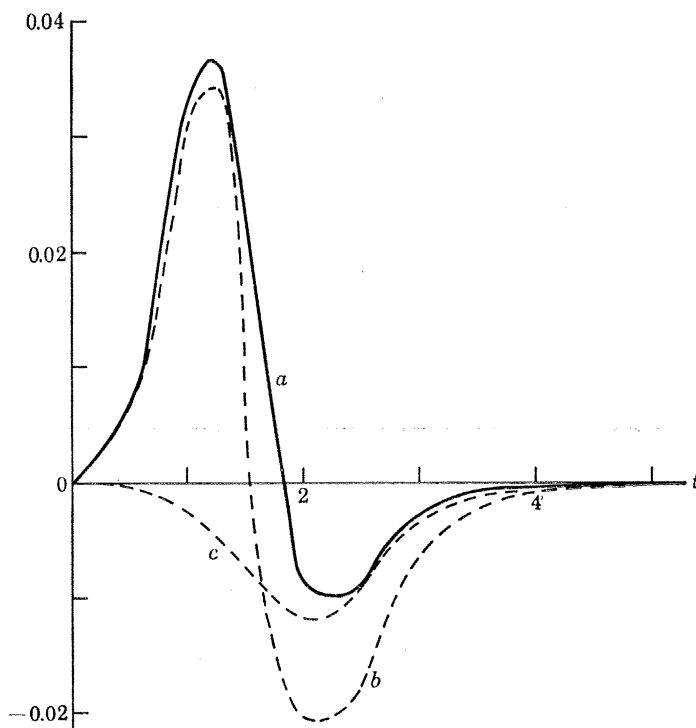
FIGURE 5. The time development of large-scale structure energy transfer mechanisms.

$$(a), \int_{-\infty}^{\infty} -\overline{\tilde{u}\tilde{w}}\frac{\partial \bar{U}}{\partial z}dz; \quad (b)\ \frac{1}{2}\frac{d}{dt}\int_{-\infty}^{\infty} \overline{(\tilde{u}^2+\tilde{w}^2)}dz; \quad (c) \int_{-\infty}^{\infty} \left[\overline{\tilde{r}_{xx}\frac{\partial \tilde{u}}{\partial x}}+\overline{\tilde{r}_{xz}\left(\frac{\partial \tilde{u}}{\partial z}+\frac{\partial \tilde{w}}{\partial x}\right)}+\overline{\tilde{r}_{zz}\frac{\partial \tilde{w}}{\partial z}}\right]dz.$$

The integral characterizing the energy transfer between the large-scale structure and the fine-grained turbulence is

$$I_{lt} = \int_{-\infty}^{\infty} -\left[\overline{\tilde{r}_{xx}\frac{\partial \tilde{u}}{\partial x}}+\overline{\tilde{r}_{xz}\left(\frac{\partial \tilde{u}}{\partial z}+\frac{\partial \tilde{w}}{\partial x}\right)}+\overline{\tilde{r}_{zz}\frac{\partial \tilde{w}}{\partial z}}\right]dz. \tag{6.9}$$

The integral of the viscous dissipation rate of the fine-grained turbulence is

$$\overline{\phi'} = \int_{-\infty}^{\infty} \bar{\epsilon}\,dz. \tag{6.10}$$

The physical interpretation of (6.3)–(6.5) has been discussed thoroughly in Liu & Merkine (1976a), who used the shape assumptions to reduce these equations to a set of equations for the energy densities of the three components of motion. The behaviour of (6.3)–(6.5) is here obtained directly from the numerical results for diagnostic purposes.

Figure 5 shows the three terms in (6.4). The large-scale structure production integral is first positive, indicating that energy is produced from the mean flow; after $t \approx 1.8$ it becomes negative, indicating that energy is fed back into the mean flow. In 'turbulence' language this latter behaviour is usually referred to as a negative (eddy) viscosity phenomenon (Starr 1968). It is, however, a phenomenon which is familiar in hydrodynamic instability and coherent structures in laminar flows both theoretically (see, for instance, Ko *et al.* 1970; Patnaik *et al.* 1976) and
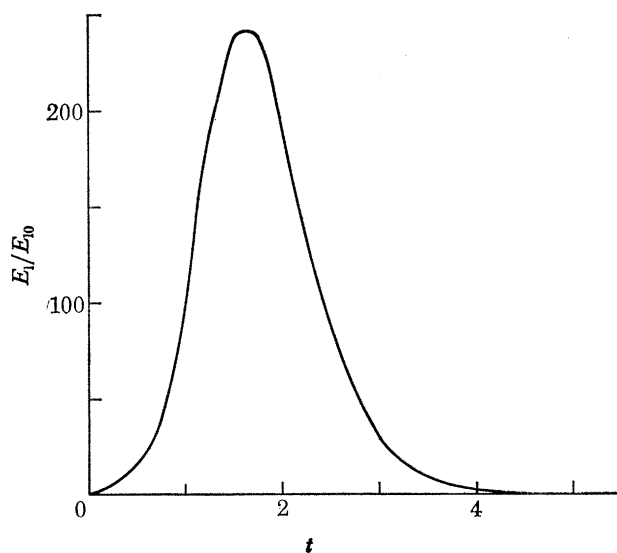
FIGURE 6. The time development of large-scale structure global kinetic energy.

experimentally (see, for instance, Durgin & Karlsson 1971). It was speculated in Liu (1971) that such inverse coherent structure production also occurs in free turbulent shear flows. It is essentially an 'inviscid' or 'dynamical' phenomenon in the hydrodynamic stability sense and can be imagined to occur even when linear stability characteristics are applied to developing shear flow by taking the hydrodynamic stability characteristics as scaled locally by the shear layer thickness. Take, for instance, the stability characteristics of figure 2. For a fixed physical wavenumber, α is scaled by the local shear layer thickness in this interpretation. As the shear layer develops, α thus increases towards the right of the diagram with increasing time; eventually the amplification rate curve αc_i would become negative and thereby produce damped disturbances, in which case energy is transferred back to the mean flow. The nonlinear numerical results here and in Patnaik *et al.* (1976) essentially bear the proper resemblance to the approximate interpretations using the kinematics of the linear theory locally. However, the dynamics of the evolution is history-dependent, and linear theory alone cannot give it.

The development of the energy transfer integral from the large-scale structure to fine-grained turbulence is also shown in figure 5. The contributions to this integral give a net energy transfer from the large-scale structure to the fine-grained turbulence, with a peak in the integral occurring during its time development. This, again, is qualitatively in agreement with the approximate calculations described in Liu & Merkine (1976a), including the peak of the corresponding quantity $(|A|^2 EI_{wt})$ with time in Liu & Merkine (1976a).

The difference of the two interaction integrals individually shown in figure 5, $\check{I}_p - I_{1t}$, then gives the time rate of change of the kinetic energy content of the large-scale structure, dE_1/dt,

shown also in figure 5. The curve crosses the axis at about $t \approx 1.50$ and thus E_1 peaks at that time. The negative region of dE_1/dt is approximately equal to the positive region and thus produces in E_1 a decay to very small values as time increases past $t \approx 5$. Note also that the production integral $\tilde{I}_p$ changes signs; thus becoming at some time a source of energy to the mean flow. The behaviour of $\tilde{I}_p$ implies that at some time the wave becomes unable to extract energy from the mean flow due to the distortion of the mean flow, as in nonlinear hydrodynamic stability theory (Stuart 1956), through the action of the Reynolds stress $\overline{\tilde{u}\tilde{w}}$. Subsequent nonlinear inter-actions causes the stresses $\overline{\tilde{u}\tilde{w}}$ to diminish and eventually change sign. Figure 6 shows the resulting E_1 plotted relative to E_{10}, with a maximum relative amplification of 250 for the case calculated.
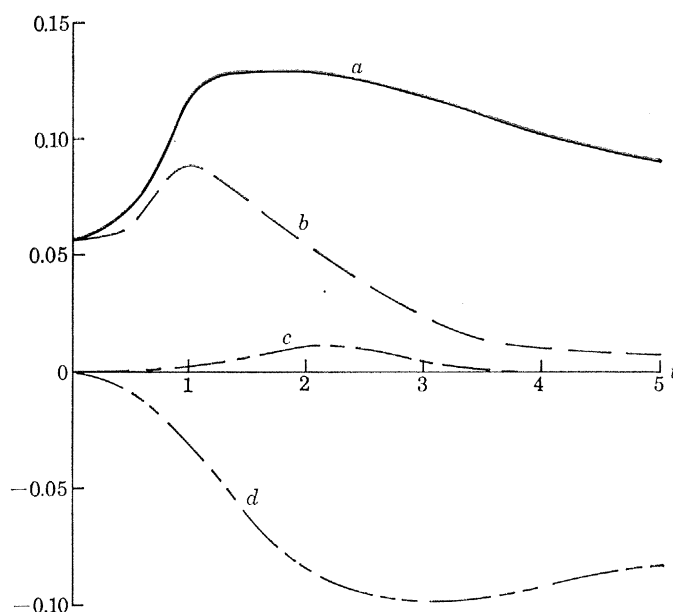

FIGURE 7. The time development of fine-grained turbulence energy transfer mechanisms.

$$(a) \int_{-\infty}^{\infty} -\overline{u'w'}\frac{\partial \overline{U}}{\partial z}\,dz; \quad (b) \frac{1}{2}\frac{d}{dt}\int_{-\infty}^{\infty} \overline{(u'^2+v'^2+w'^2)}\,dz; \quad (c) \int_{-\infty}^{\infty} -\left[\overline{\tilde{\tau}_{xx}\frac{\partial \tilde{u}}{\partial x}}+\overline{\tilde{\tau}_{xz}\left(\frac{\partial \tilde{u}}{\partial z}+\frac{\partial \tilde{u}}{\partial x}\right)}+\overline{\tilde{\tau}_{zz}\frac{\partial \tilde{w}}{\partial z}}\right]\,dz;$$

$$(d) -\int_{-\infty}^{\infty} \bar{e}\,dz.$$

The four terms of (6.5) are shown in figure 7. In the computed initial self-preserving shear flow the fine-grained turbulence production integral I_p' is slightly larger than the viscous dissipation integral $\overline{\phi'}$ and this accounts for the initial small rate of growth of the turbulent kinetic energy integral E_t. However, the large-scale structure, which subsequently develops, produces such a modification of the Reynolds-mean flow, and through distortion of the velocity profile and spreading, than an implicit enhancement of the fine-grained turbulence production takes place. After a period of initial readjustment, I_p' and $\overline{\phi'}$ nearly balance each other at later times, so that the rate of change of the turbulence energy content dE_t/dt eventually becomes small again and E_t, shown in figure 8, develops slowly in a manner resembling its initial development. The interaction between the large-scale structure and turbulence takes place earlier. Because of the relatively small initial large-scale structure energy level, $E_{10}/E_{t0} \approx 10^{-2}$, the large-scale structure does not contribute significantly to the direct development of turbulence energy. In this case, that development is attributed primarily to the imbalance between production from the mean

and viscous dissipation, although the time integral of the bump I_{1t} does make a finite contribution to the quasi-equilibrium level achieved by E_t in figure 8. The qualitative behaviour of E_1 and E_t, including the contributing physical mechanisms, is entirely similar to that derived from the earlier approximate considerations (Liu & Merkine 1976 a; Liu & Alper 1977; Alper & Liu 1978).

The time rate of decrease of the mean energy defect E_m is governed by $-(\tilde{I}_p + I'_p)$, where $\tilde{I}_p$ and I'_p are shown in figures 5 and 7, respectively. The total energy of the entire system $E_m + E_1 + E_t$, formed by the sum of (6.3)–(6.5), decreases in time according to the viscous dissipation rate of the smaller eddies ϕ'.
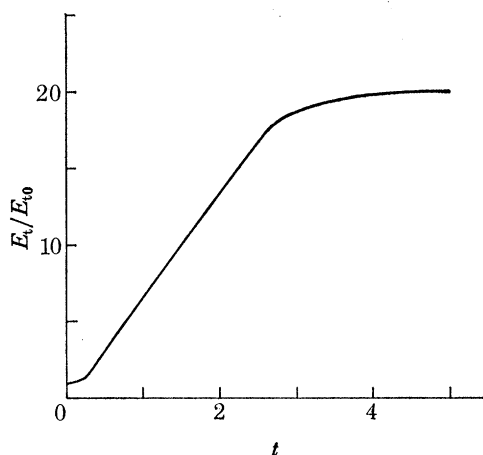
FIGURE 8. The time development of fine-grained turbulence global kinetic energy.

Of interest are the detailed spatial contributions to I_{1t}, defined in (6.9). The various terms in the integrand of I_{1t} are shown in figure 9 for the instant $t = 1.50$ when E_1 reaches its maximum. The lower half of the vertical axis implies transfer of energy from the fine-grained turbulence to the large-scale structure on the (horizontal) average, while the opposite is true in the upper half of the vertical axis; for instance, both $-\overline{\tilde{r}_{xz}\partial\tilde{u}/\partial z}$ and $-\overline{\tilde{r}_{xx}\partial\tilde{u}/\partial x}$ contribute to transfer of energy from the fine-grained turbulence to the large-scale structure in certain regions across the shear layer. However, these contributions are offset by the energy transfer from the large-scale structure to the finer scales contributed by the other shear and normal stress mechanisms, predominantly $-\overline{\tilde{r}_{xz}\partial\tilde{w}/\partial x}$ and $-\overline{\tilde{r}_{zz}\partial\tilde{w}/\partial z}$. The contributions from the various transfer mechanisms bring about a net energy transfer from the large to the finer scales of motion, as indicated by the dashed line in figure 9. The same conclusion was reached in the approximate analysis of Liu & Merkine (1976 a). Their distribution for $-\overline{\tilde{r}_{ij}\partial\tilde{u}_i/\partial x_j}$ was obtained from approximate calculations using the linear theory and their particular numerical illustration was for the most-amplified mode, and was thus somewhat similar to the initial condition situation in the present calculations. Figure 9 here is for $t = 1.50$ when considerable nonlinear interactions have taken place, including shifts in phase (as an examination of the vorticity contours in figure 4 here shows); it is therefore not expected that the details of the individual distributions of $-\overline{\tilde{r}_{ij}\partial\tilde{u}_i/\partial x_j}$ given here should bear any detailed resemblance to those given in Liu & Merkine (1976 a). However, that $-\overline{\tilde{r}_{ij}\partial\tilde{u}_i/\partial x_j}$ does indeed contribute to a transfer of energy from the fine to the large-scale in certain regions of the shear layer is in agreement with the approximate considerations there. The net effect, that energy is transferred from the large to the fine scales,

is of course in general agreement, as pointed out earlier. The determination of the mechanisms and directions of this energy transfer in previous work (Liu & Merkine 1976a; Alper & Liu 1978) and in the present work according to the conservation laws is, we believe, a significant contribution to the understanding of the interaction between large-scale coherent structures and fine-grained random turbulence.
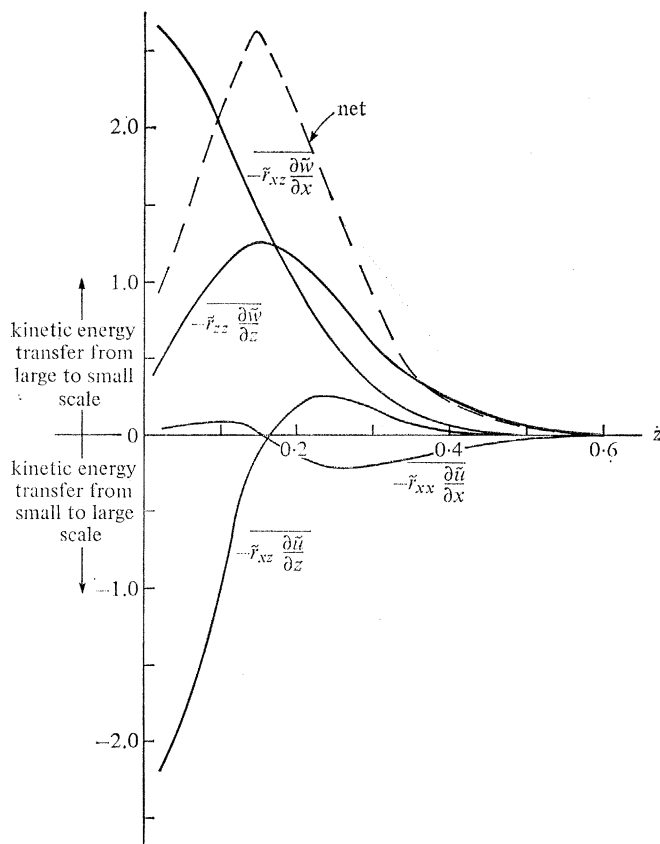

FIGURE 9. The vertical distributions of energy transfer mechanisms between the large-scale structure and fine-grained turbulence at $t = 1.50$.

The numerical integrations were carried out over the time scale of a single amplification–decay process (figure 5). We did not carry out further integrations beyond this to see whether repeated 'bursts' (Liu & Merkine 1976a) occurred. However, in their approximate analyses Liu & Merkine (1976a) found such repeated bursts only for initially nearly neutral disturbances, not for the initially most-amplified mode (the mode we deal with here).

The mean shear layer thickness δ, (normalized by the initial thickness), defined by (4.1), is shown in figure 10. It reaches one of constant slope when E_t essentially saturates. Also shown in figure 10 is an estimated overall dissipation length scale of the fine-grained turbulence $L_\epsilon \approx E_t^{\frac{3}{2}}/\overline{\phi'}$ normalized by its initial value $L_{\epsilon 0} = (\frac{2}{3}E_{t0})^{\frac{3}{2}}/\overline{\phi'_0} \approx 1.355$. Since $L_{\epsilon 0}$ is referred to δ_0 and the total width of the shear layer is about $3\delta_0$, the initial dissipation length scale of the self-preserving shear flow is about 0.45 the total shear layer width. After the start of the large-scale structure and fine-grained turbulence interaction, there is a rapid production of the finer scales indicated by the dip in $L_\epsilon/L_{\epsilon 0}$ in figure 10. This is accompanied by a rapid rise of the vertical extent of the

large-scale structure closed-streamline H, normalized by its initial value H_0. As H/H_0 eventually declines, $L_\epsilon/L_{\epsilon 0}$ rises indicating that the fine-grained turbulence scales eventually become larger. However, the ratio L_ϵ/δ, shown also in figure 10, eventually remains very nearly constant. A close examination of the 'graininess' of the turbulence in Brown & Roshko's (1974) observations indeed shows such a feature, that the downstream spread of the shear layer is accompanied by a coarsing of the graininess.
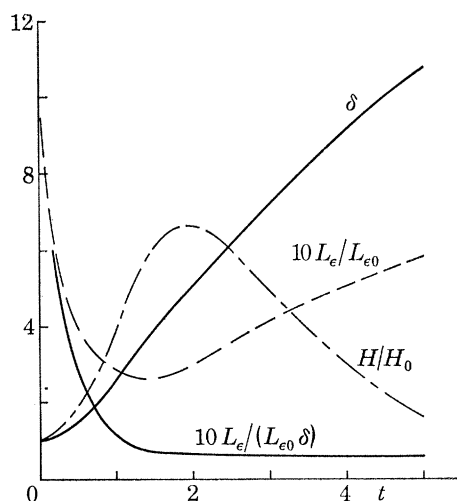
FIGURE 10. The development of shear layer thickness and fine-grained turbulence dissipation length scale.

(c) The structure of conditionally averaged turbulent stresses and their production mechanisms

In § 6 (b) we performed horizontal averaging upon certain of the numerical results in order to bring out the interactions in the mean between the large-scale structure, the fine-grained turbulence and the mean flow. Now in the formulation for the numerical calculation the large-scale coherent motion is represented by the quantity U_i which includes both the mean $\bar{U}_i$ and the large-scale oscillations $\tilde{u}_i$ with zero mean. The conditional average of the total flow quantity $u_i = U_i + u_i'$, with u_i' the fine-grained turbulence, produces just U_i. We recall that the turbulent stresses are subject to such an averaging procedure as well. Thus the conditionally averaged turbulent stresses $\langle u_i' u_j' \rangle$, like U_i, include both a mean $\overline{u_i' u_j'}$ part and a large-scale-modulated stress $\tilde{r}_{ij}$ which also has zero mean. In this section we shall look at the spatial structure of the conditionally averaged stresses $\langle u_i' u_j' \rangle$, which includes the components of the kinetic energy $\langle k \rangle = \frac{1}{2}\langle u_i' u_i' \rangle$, and the mechanisms for their production from the conditionally averaged flow U_i. This point of view, which bypasses the introduction of an explicit Reynolds-type horizontally averaged mean flow, arises directly from the numerical results and is one which is probably favoured by experimentalists studying coherent structures in turbulence by using conditional sampling techniques (Kovasznay et al. 1970). In this case, U_i is regarded as the local 'mean flow' and $\langle u_i' u_j' \rangle$ as the 'turbulence.' The physical implications of this point of view and its connection with the traditional Reynolds-type averaging have been thoroughly discussed throughout in this paper.

The structure of $\frac{1}{2}\langle u'^2 \rangle$ is shown in figure 11 (a) at $t = 1.50$ when E_1 has reached its maximal value. It appears to be concentrated horizontally at the extremities of the wavelength and
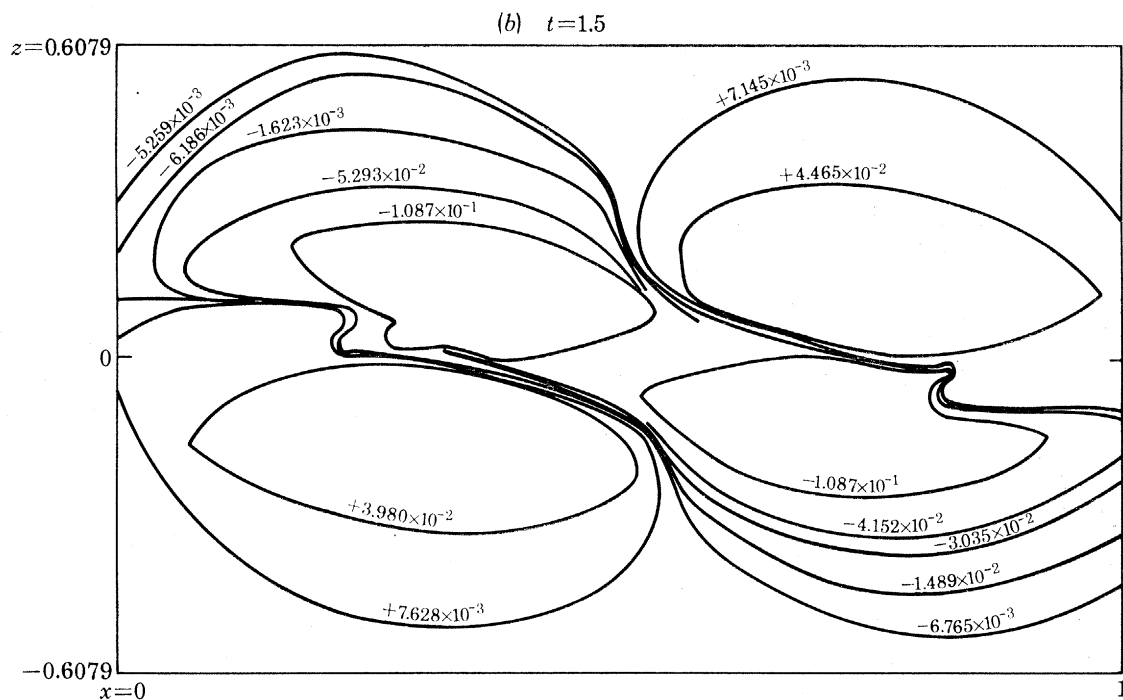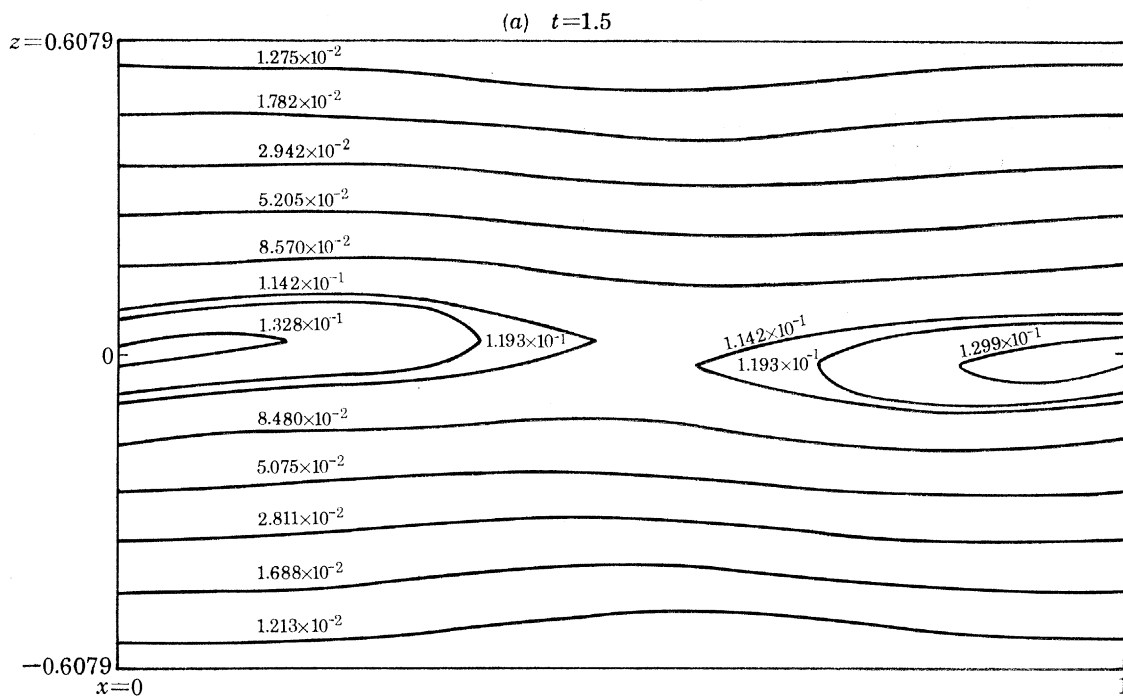
(a) t=1.5

(b) t=1.5
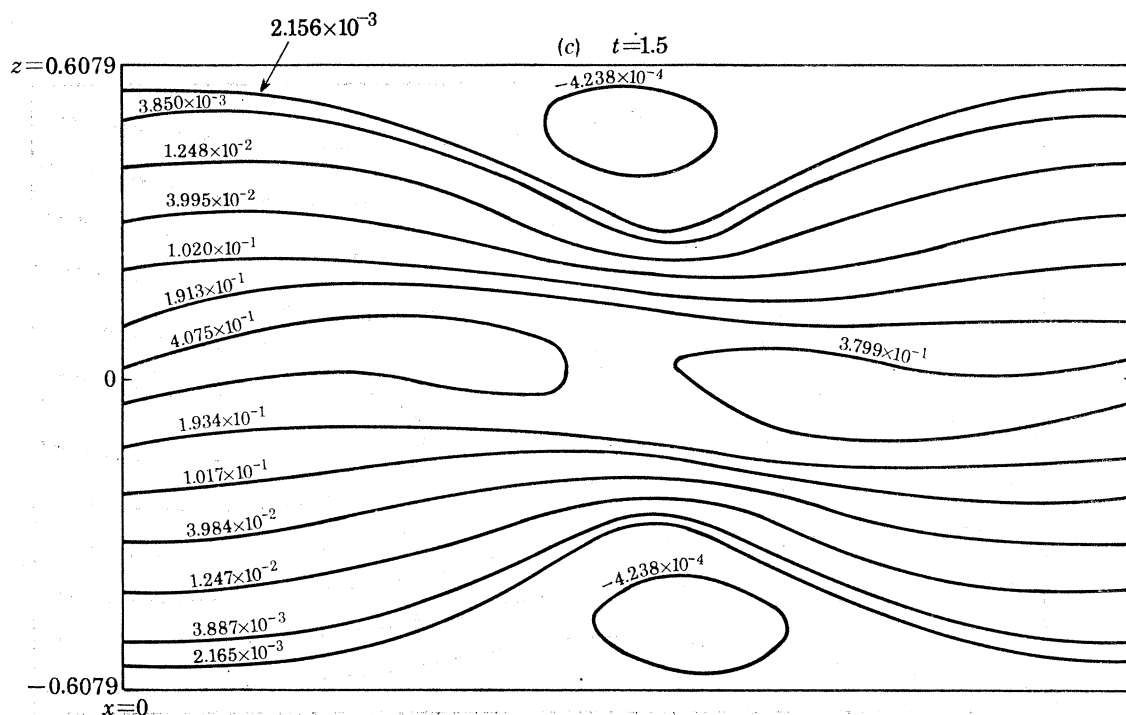

FIGURE 11a AND b. For description see opposite.

FIGURE 11. The horizontal component of conditionally averaged turbulence kinetic energy and its production mechanisms at $t = 1.50$. (a) $\frac{1}{2}\langle u'^2 \rangle$. (b) Normal stress production rate, $-\langle u'^2 \rangle \partial U/\partial x$. (c) Shear stress production rate, $-\langle u'w' \rangle \partial U/\partial z$.

vertically at the centre of the shear layer. The production mechanisms for $\frac{1}{2}\langle u'^2 \rangle$ via the work done by the normal and shear stresses, $-\langle u'^2 \rangle$ and $-\langle u'w' \rangle$, against the velocity gradients of the conditionally averaged flow, $\partial U/\partial x$ and $\partial U/\partial z$, respectively are shown in figures 11 (b) and (c). The dominant production mechanism is that due to the shear stress, $-\langle u'w' \rangle$, in combination with the rate of shear strain $\partial U/\partial z$. The contours of $\frac{1}{2}\langle u'^2 \rangle$ (figure 11a) are qualitatively similar in shape to those of $-\langle u'w' \rangle \partial U/\partial x$ (figure 11c). At the vertical outer edges and horizontally in the centre of the shear layer there are concentrated local pockets in which energy is transferred from the turbulence to the conditionally averaged flow. Although this transfer rate is relatively small in magnitude, its tendency is to depress the constant $\frac{1}{2}\langle u'^2 \rangle$ contours at the outer regions of the shear layer. In examining the contours of $-\langle u'^2 \rangle \partial U/\partial x$ in figure 11 (b), we see that in the upper left and lower right regions of the coherent structure energy is transferred from the turbulence back to U, while the opposite is true for the upper right and lower left regions of the structure. This would have a tendency to rotate the $\frac{1}{2}\langle u'^2 \rangle$ contours in an anticlockwise direction in figure 11 (a). However, this is very nearly offset by the opposite, clockwise tendency of the stronger production mechanism $-\langle u'w' \rangle \partial U/\partial z$ shown in figure 11 (c).

The contour of one half the conditionally averaged vertical stress $\frac{1}{2}\langle w'^2 \rangle$ is shown in figure 12 (a), also at $t = 1.50$. It is qualitatively similar in shape to $\frac{1}{2}\langle u'^2 \rangle$ but has about half its value. The energy transfer mechanisms from the conditionally averaged flow structure W are $-\langle w'^2 \rangle \partial W/\partial z$ and $-\langle u'w' \rangle \partial W/\partial x$, shown in figures 12 (b) and 12 (c), respectively. They are qualitatively different but are of the same relative strength. The normal stress–strain mechanism, $-\langle w'^2 \rangle \partial W/\partial z$, tends to depress the $\frac{1}{2}\langle w'^2 \rangle$ contours (figure 12a) in the right horizontal region and elevate them in the left region, as is evident from figure 12 (a). The normal stress–strain
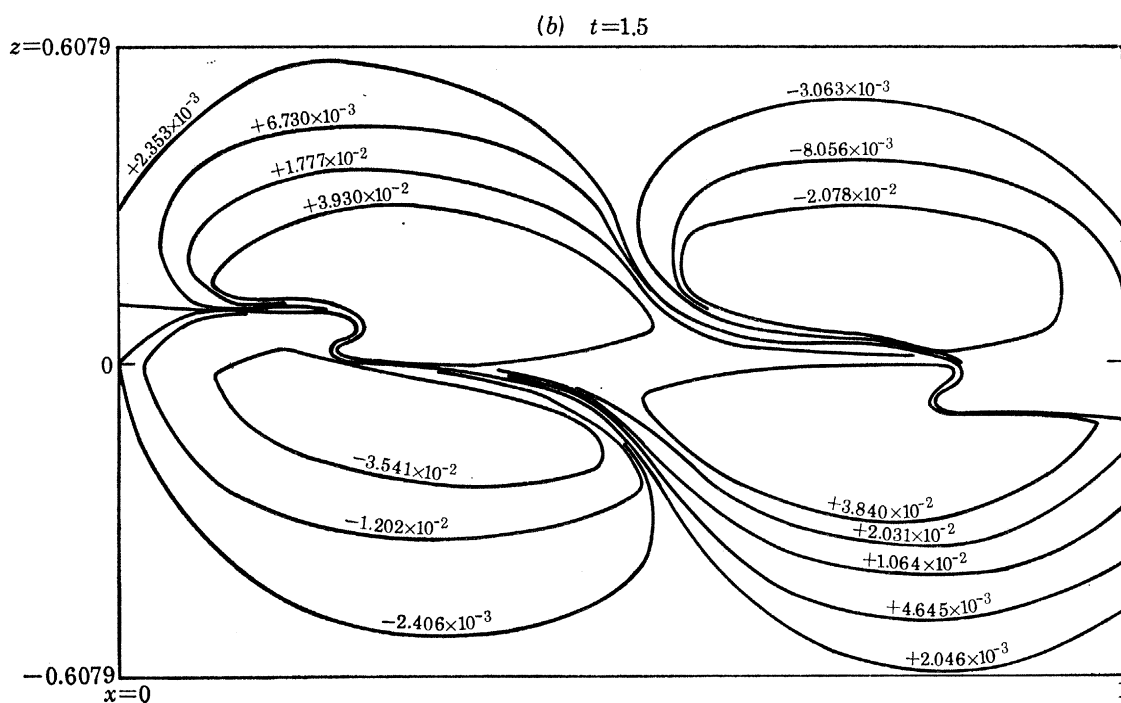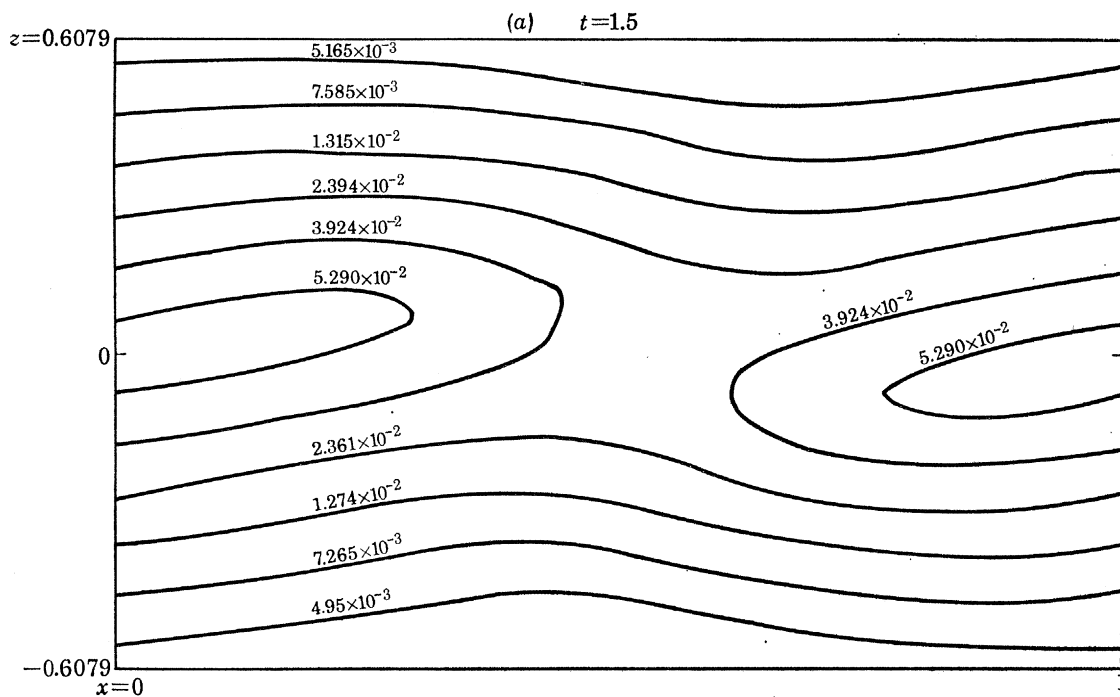
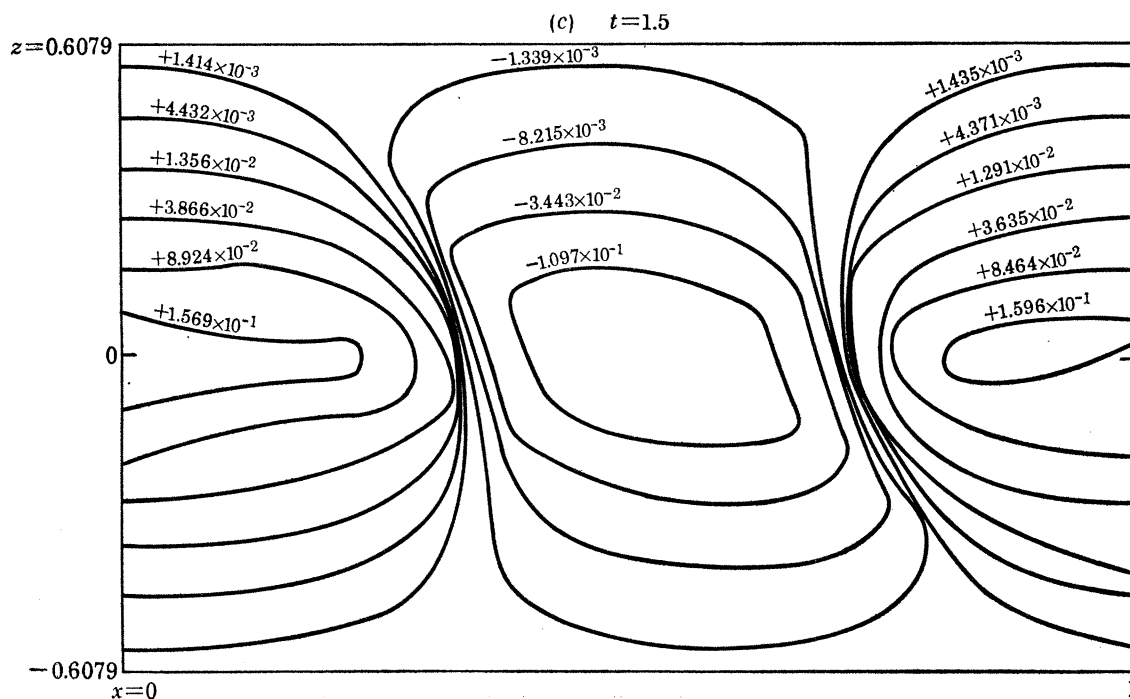FIGURE 12a AND b. For description see opposite.

FIGURE 12. The vertical component of conditionally averaged turbulence kinetic energy and its production mechanisms at $t = 1.50$. (a) $\frac{1}{2}\langle w'^2 \rangle$. (b) Normal stress production rate, $-\langle w'^2 \rangle \partial W / \partial z$. (c) Shear stress production rate, $-\langle u'w' \rangle \partial W / \partial x$.

mechanism gives an approximately zero conversion at the centre of the shear layer, and the structure of $\frac{1}{2}\langle w'^2 \rangle$ there must be accounted for by the shear stress–strain conversion mechanism (figure 12 c), which is indeed what happens at the horizontal extremities of the structure. There is a large closed cell at the centre, filling the vertical extent of the shear layer, which converts energy back to the W flow. This would account for the depression of the $\frac{1}{2}\langle w'^2 \rangle$ lines in that region.

The existence of $\frac{1}{2}\langle u'^2 \rangle$ and $\frac{1}{2}\langle w'^2 \rangle$ is *primarily* attributed to their respective production mechanisms. Their detailed shapes, of course, must finally be accounted for by the balance with the diffusion mechanisms of the triple correlations, the pressure–velocity redistribution and, of course, the viscous dissipation rate. The conditionally averaged dissipation $\langle \epsilon \rangle$ and shear stress $-\langle u'w' \rangle$ qualitatively follow the contours of $\frac{1}{2}\langle u'^2 \rangle$ and $\frac{1}{2}\langle w'^2 \rangle$ and are therefore not shown here.

Figure 13 (a) shows the contours of the conditionally averaged spanwise contribution to the kinetic energy $\frac{1}{2}\langle v'^2 \rangle$. In this problem the large-scale structure is two dimensional, and spanwise gradients of all conditionally averaged quantities vanish. There is therefore no direct production of $\frac{1}{2}\langle v'^2 \rangle$ by the large-scale structure. There is, however, an indirect production via the approximated form of the pressure–velocity strain correlation which redistributes the energy from $\frac{1}{2}\langle u'^2 \rangle$ and $\frac{1}{2}\langle w'^2 \rangle$ to $\frac{1}{2}\langle v'^2 \rangle$. The pressure–velocity strain correlation $\langle p' \partial v' / \partial y \rangle$ shown in figure 13 (b), essentially accounts for the contours of $\frac{1}{2}\langle v'^2 \rangle$ of figure 13 (a). This consideration illustrates how three dimensional fine-grained turbulence is indirectly produced from a large-scale two dimensional coherent structure.
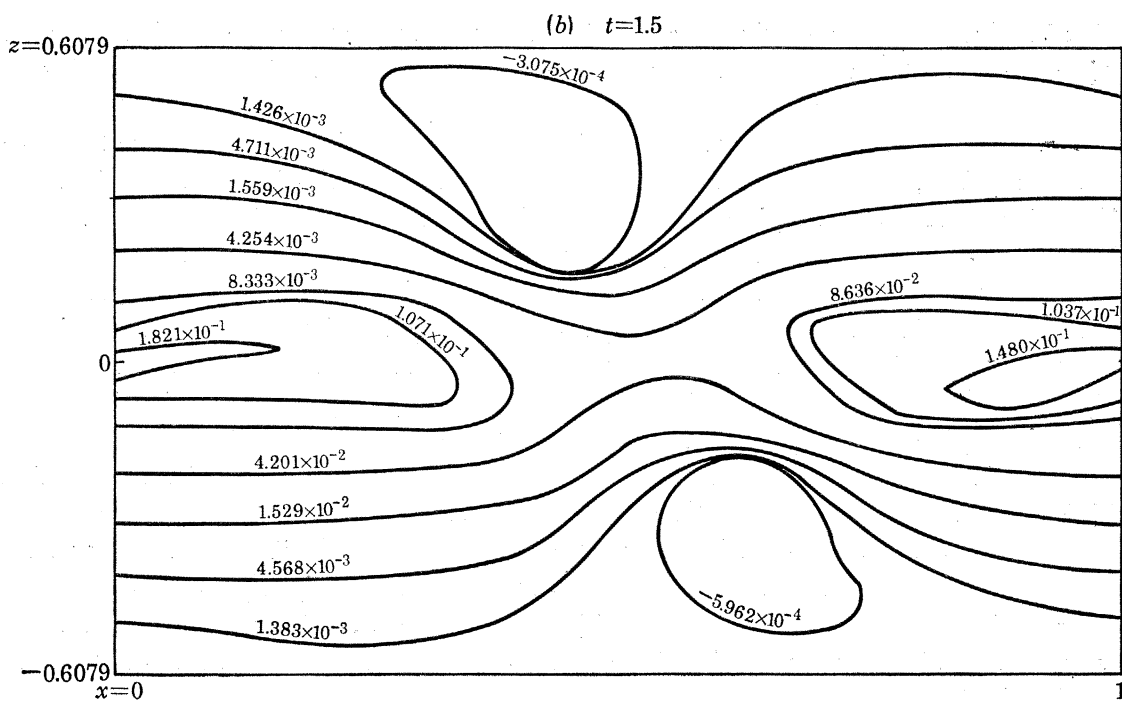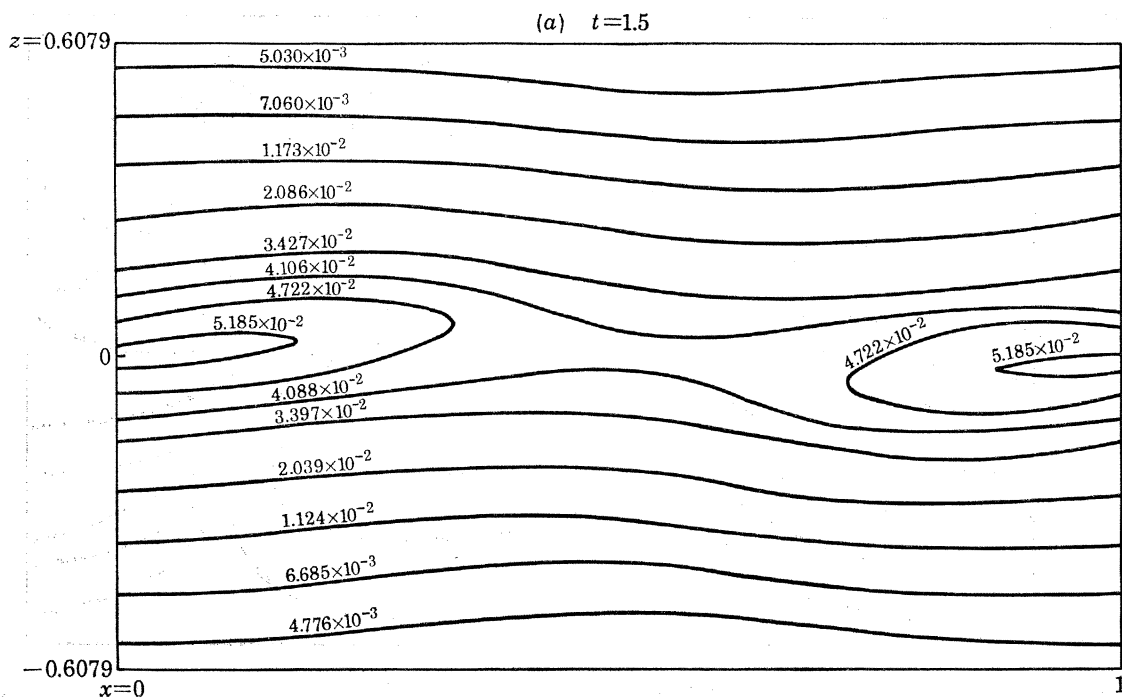
FIGURE 13. The spanwise component of conditionally averaged turbulence kinetic energy and its 'production' mechanism at $t = 1.50$. (a) $\frac{1}{2}\langle v'^2 \rangle$. (b) Pressure–velocity strain redistribution, $\langle p' \partial v'/\partial y \rangle$, according to the closure approximation; $\langle p' \partial v'/\partial y \rangle \approx -\frac{1}{2}c_1(\langle \epsilon \rangle/\langle k \rangle)[\langle v'^2 \rangle - \frac{2}{3}\langle k \rangle] - \frac{1}{2}\gamma[\langle P_{22} \rangle - \frac{1}{3}\langle P_{kk} \rangle]$.

7. Further discussions

The numerical work reported in this paper complements our previous work on similar problems by means of approximate integral energy considerations (Liu & Merkine 1976 a; Alper & Liu 1978). In the present work the temporal interactions in the mean are considered and the mean flow is homogeneous horizontally and its overall evolution is in time. In the real laboratory problem the mean shear layer develops with the downstream distance. The former problem was chosen for our numerical work because it bears a remarkable physical resemblance to the spatially developing problem but lacks the conceptual numerical difficulties involved in specifying the downstream conditions in the presence of coherent structures and turbulence. There is, of course, no obvious direct one-to-one correspondence between the two problems, as was discussed earlier (Alper & Liu 1978). In making inferences from the present temporal problem to the spatial problem, the time here corresponds to the downstream distance and the wavenumber here corresponds to the frequency in the spatial problem. The conditional average in the latter is then linked to the phase of the imposed disturbance upstream and such (phase) averages are fully realizable in the laboratory (Binder & Favre-Marinet 1973; Hussain & Reynolds 1970; Kendall 1970; Favre-Martinet 1975). The Reynolds average, which is the horizontal average in this work, would be the time average in the spatial problem.

Although the present work furnishes the local structural details of the problem, the overall interaction process is still governed by the 'global' energy exchange processes. The mechanisms for such global exchange processes, which were discussed in the approximate analysis (Liu & Merkine 1976 a; Liu & Alper 1977; Alper & Liu 1978), are recovered here via Reynolds averaging of certain of the details of the problem. The global energies E_l and E_t essentially govern the amplitude of the large-scale coherent structure and the fine-grained turbulence. That E_l amplifies and decays indicates that its interaction with the turbulence and the mean flow is a *non-equilibrium* process and, as such, is dependent upon the initial conditions. It is the initial imbalance between its production from the mean and its 'dissipation' by the fine-grained turbulence that allows its dramatic growth. In the latter half of its life cycle the reverse is true. The fine-grained turbulence rises from an initial quasi-equilibrium level to a new one at the end of this non-equilibrium interaction, because it extracts far more energy from the mean flow and from the large-scale structure than it loses through viscous dissipation. The energy gained from the large-scale structure is, of course, extracted indirectly from the mean flow. The direct production of turbulence from the mean flow may also be enhanced by the local distortions of the mean flow by the large-scale structure. In order to understand the role of large-scale structures in turbulent shear flows, we have thus found that it is essential to consider the overall non-equilibrium energy exchange processes. The present numerical results enable us to describe the qualitative principles in the evolution of the problem. The relevant detailed structure of the problem, particularly, say, at maximal large-scale structure intensities, must be placed in the perspective of the developing events described by the global considerations.

It is of interest to discuss, in the light of the present numerical results, attempts at a nonlinear critical layer analysis of the same problem making use of ideas similar to those of Benny & Bergeron (1969), with an appropriately defined turbulent Reynolds number and augmented by the stress equations for $\tilde{r}_{ij}$. The nonlinear critical layer analysis requires a neutral (or nearly neutral) condition with the large-scale structure being small (though nonlinear). With respect to the present numerical results, such an analysis would most probably suit a situation in the

latter stages of the development ($t \gtrsim 5.0$) when the amplitude is small and the conditions nearly 'neutral.' The small amplitude requirement precludes placing the nonlinear critical layer at the time $t \approx 1.5$; and, although there the large-scale structure is 'neutral', it is not a steady situation. The nonlinear critical layer theory also requires that the vorticity within the cats' eye pattern be uniform. The numerical results here show, however, that because of strong interactions with the mean flow and turbulence, the large-scale structure vorticity is distributed rather unevenly within the cats' eye.

In a real, natural turbulent shear layer in the laboratory it is not inconceivable that a spectrum of disturbances exists upstream of the free shear flow. This situation is made all the more likely if the upstream boundary layers are turbulent. The free shear layer, which is inflexional in its mean velocity profile, selects from the initial broad-band disturbances the mode (or narrow band of modes) that is most efficient in extracting energy from the mean flow relative to the rate of 'dissipation' by the eddies of much smaller scale. Because of the initial broad-band disturbances, the subsequent observed large-scale structure development is dispersive about, rather than concentrated upon, the initially most efficient mode. It is likely that, contained in the initial broad-band disturbances, are disturbances whose frequencies are 'subharmonic' relative to the most efficient mode. Given an opportune phase relation between the subharmonic and the fundamental component, neighbouring eddies of the latter are likely to agglomerate to form a single larger-scale disturbance.† This subharmonic formation, which is familiar in transitional laminar free shear layers (Freymuth 1966; Browand 1966; Kelly 1967; Miksad 1972, 1973) is found to occur also in turbulent shear layers at relatively low Reynolds number (Winant & Browand 1974; Browand & Weidman 1976) as well as at high Reynolds numbers (Roshko 1976), including the tripling of large-scale structures. In turbulent shear layers with high Reynolds number, where the large-scale structures are superposed upon fine-grained turbulence, it is reported (Dimotakis & Brown 1976) that the production of more energetic fine-grained turbulence, not the agglomeration process, appears to be the dominant mechanism in bringing about the eventual disappearance of the large-scale structures. The observational problem is still a difficult one because of the natural, uncontrolled initial disturbances upstream.

From theoretical considerations the *initial conditions* on the interactions between the large-scale structure and fine-grained turbulence and the entire development of the shear layers enter into the problem in the form of (1) the relative initial energy levels of the large-scale coherent structure and the fine-grained turbulence, and (2) the initial mode of the large-scale structure characterized by the dimensionless wavenumber for the temporal problem and the dimensionless frequency for the spatial problem, both scaled by the initial shear layer thickness. The effects of parametric variations of initial conditions have received thorough discussion in previous theoretical studies (Liu 1971, 1974; Liu & Merkine 1976*a*; Liu & Alper 1977; Alper & Liu 1978). It is increasingly evident from observations that initial conditions do indeed also play an important role in the subsequent development of turbulent shear flows with high Reynolds number (Bradshaw 1966; Binder & Favre-Marinet 1973; Batt 1975; Favre-Marinet 1975; Laufer 1975; Dimotakis & Brown 1976; Roshko 1976; Moore 1977; Oster *et al.* 1977). In this case it is well worth repeating the suggestion, made by Liepmann (1964) some time ago, that in the experimental study of large-scale structures in free turbulent shear flows, *well controlled* disturbances be imposed in the same spirit as that of Schubauer & Skramstad's (1948) study of Tollmein–

---

† A study of this agglomeration process and its effect on the generation of turbulence, with the use of the present computational framework, is in progress.

Schlichting–Dryden waves in laminar flows. 'Well controlled' is here interpreted as the quantitative specification of the initial conditions in terms of initial energy levels, large-scale structure modes and the mean properties of the initial shear layer. Conditional sampling techniques are by no means unique and not all are necessarily susceptible to physical interpretation via conservation principles. However, the conditional averages discussed here in terms of phase averages have the advantage in connection with well-controlled disturbances that they yield results that can be interpreted through the conservation equations.

We have shown (in figure 13) how three dimensional fine-grained turbulence can be produced indirectly from the two dimensional large-scale structure via the isotropizing process of the approximated pressure–strain correlation. Spanwise periodicity in the large-scale structure has been recently observed by Konrad (1976). There is then the additional possibility that three dimensional fine-grained turbulence can also be produced directly from the spanwise periodicity. The role of such 'three-dimensional' large-scale coherent structures in the production of turbulence warrants further studies.

REFERENCES

Alper, A. & Liu, J. T. C. 1978 On the interactions between large-scale structure and fine-grained turbulence in a free shear flow. II. The development of spatial interactions in the mean. *Proc. R. Soc. Lond.* A **359**, 497.

Amsden, A. A. & Harlow, F. H. 1964 Slip instability. *Phys. Fluids* **7**, 327.

Batt, R. G. 1975 Some measurements on the effect of tripping the two-dimensional shear layer. *AIAA Jl.* **13**, 245.

Benny, D. J. & Bergeron, R. F. Jr 1969 A new class of nonlinear waves in parallel flows. *Stud. appl. Math.* **48**, 181.

Binder, G. & Favre-Marinet, M. 1973 Mixing improvement in pulsating turbulent jets. In *Fluid mechanics of mixing* (ed. E. M. Uram & V. W. Goldschmidt), pp. 167–172. New York: A.S.M.E.

Bradshaw, P. 1972 The understanding and prediction of turbulent flow. *Aeronaut. J.* **76**, 403.

Bradshaw, P. 1966 The effect of initial conditions on the development of a free shear layer. *J. Fluid Mech.* **26**, 225.

Browand, F. K. 1966 An experimental investigation of the instability of an incompressible, separated shear layer. *J. Fluid Mech.* **26**, 281.

Browand, F. K. & Weidman, P. D. 1976 Large scales in the developing mixing layer. *J. Fluid Mech.* **76**, 127.

Chou, P. Y. 1945 On velocity correlations and the solutions of the equations of turbulent fluctuation. *Q. appl. Math.* **3**, 38.

Daly, B. J. & Harlow, F. H. 1970 Transport equations of turbulence. *Phys. Fluids* **13**, 2634.

Dimotakis, P. E. & Brown, G. L. 1976 The mixing layer at high Reynolds number: large-structure dynamics and entrainment. *J. Fluid Mech.* **78**, 535.

Durgin, W. W. & Karlsson, S. K. F. 1971 On the phenomenon of vortex street breakdown. *J. Fluid Mech.* **48**, 507.

Favre-Marinet, M. 1975 Structure des jets pulsants. Docteur-Ingénieur Thèse, L'Université Scientifique et Médicale de Grenoble. (see also Favre-Marinet, M. & Binder, G. 1979 *J. Méchanique* **18**, 365).

Freymuth, P. 1966 On transition in a separated boundary layer. *J. Fluid Mech.* **25**, 683.

Gatski, T. B. & Liu, J. T. C. 1977 Numerical solution for the large-scale coherent structure in a turbulent shear layer. Abstract in *Bull. Am. phys. Soc.* **22**, 1284.

Hanjalić, K. & Launder, B. E. 1972 A Reynolds stress model of turbulence and its application to thin shear flows. *J. Fluid Mech.* **52**, 609.

Hussain, A. K. M. F. & Reynolds, W. C. 1970 The mechanics of an organized wave in turbulent shear flow. *J. Fluid Mech.* **41**, 241.

Kelly, R. E. 1967 On the stability of an inviscid shear layer which is periodic in space and time. *J. Fluid Mech.* **27**, 657.

Kendall, J. M. 1970 The turbulent boundary layer over a wall with progressive surface waves. *J. Fluid Mech.* **41**, 259.

Ko, D. R. S., Kubota, T. & Lees, L. 1970 Finite disturbance effect in the stability of a laminar incompressible wake behind a flat plate. *J. Fluid Mech.* **40**, 315.

Konrad, J. H. 1976 An experimental investigation of mixing in two-dimensional turbulent shear flows with applications to diffusion limited chemical reactions. *Project SQUID Tech. Rep.* CIT-8-PU, California Institute of Technology.

Kovasznay, L. S. G., Kibens, V. & Blackwelder, R. F. 1970 Large-scale motion in the intermittent region of a turbulent boundary layer. *J. Fluid Mech.* **41**, 283.

Laufer, J. 1975 New trends in experimental turbulence research. In *A. Rev. Fluid Mech.* **7**, 307.

Launder, B. E., Reece, G. J. & Rodi, W. 1975 Progress in the development of a Reynolds-stress turbulence closure. *J. Fluid Mech.* **68**, 537.

Liepmann, H. W. 1964 Free turbulent flows. In *The mechanics of turbulence*, pp. 211–227. *Int. Symp. nat. Sci. Res. Centre*, Marseille 1961. New York: Gordon & Breach.

Liepmann, H. W. & Laufer, J. 1947 Investigation of free turbulent mixing. *Tech. Notes natn. advis. Comm. Aeronaut.*, *Washington*, no. 1257.

Lin, C. C. 1955 *The theory of hydrodynamic stability*. Cambridge University Press.

Liu, J. T. C. 1971 Nonlinear development of an instability wave in a turbulent wake. *Phys. Fluids* **14**, 2251.

Liu, J. T. C. 1974 Developing large-scale wavelike eddies and the near jet noise field. *J. Fluid Mech.* **62**, 437.

Liu, J. T. C. & Alper, A. 1977 On the large-scale structure in turbulent free shear flows. In *Proc. Symp. Turbulent Shear Flows*, pp. 11.1–11.11. Pennsylvania State University.

Liu, J. T. C., Alper, A. & Mankbadi, R. 1977 The large-scale organized structure in free turbulent shear flow and its radiation properties. In *Structure and mechanisms of turbulence* II (ed. H. E. Fiedler), pp. 202–218. Berlin: Springer–Verlag.

Liu, J. T. C. & Gururaj, P. M. 1974 Finite-amplitude instability of the compressible laminar wake: comparison with experiments. *Phys. Fluids* **17**, 532.

Liu, J. T. C. & Lees, L. 1970 Finite amplitude instability of the compressible laminar wake: strongly amplified disturbances. *Phys. Fluids* **13**, 2932.

Liu, J. T. C. & Merkine, L. 1976a On the interactions between large-scale structure and fine-grained turbulence in a free shear flow. I. The development of temporal interactions in the mean. *Proc. R. Soc. Lond.* A **352**, 213.

Liu, J. T. C. & Merkine, L. 1976b Energy integral description of the development of Kelvin–Helmholtz billows. *Tellus* **28**, 197.

Lumley, J. L. 1970 Toward a turbulent constitutive relation. *J. Fluid Mech.* **41**, 413.

MacPhail, D. C. 1941 Turbulence in a distorted passage and between rotating cylinders. Ph.D. dissertation, University of Cambridge.

Michalke, A. 1964 On the inviscid instability of the hyperbolic-tangent velocity profile. *J. Fluid Mech.* **19**, 543.

Michalke, A. 1965 Vortex formation in a free boundary layer according to stability theory. *J. Fluid Mech.* **22**, 371.

Miksad, R. W. 1972 Experiments on the nonlinear stages of free shear-layer transition. *J. Fluid Mech.* **56**, 695.

Miksad, R. W. 1973 Experiments on nonlinear interactions in the transition of a free shear layer. *J. Fluid Mech.* **59**, 1.

Moore, C. J. 1977 The role of shear-layer instability waves in jet exhaust noise. *J. Fluid Mech.* **80**, 321.

Monin, A. S. & Yaglom, A. M. 1971 *Statistical fluid mechanics: mechanics of turbulence*, vol. I. Massachusetts Institute of Technology Press.

Oster, D., Dziomba, B., Fiedler, H. E. & Wygnanski, I. 1977 On the effect of initial conditions on the two-dimensional turbulent mixing layer. In *Structure and mechanisms of turbulence* I (ed. H. E. Fiedler), pp. 48–64. Berlin: Springer–Verlag.

Pai, S. I. 1939 Turbulent flow between rotating cylinders. Ph.D. dissertation, California Institute of Technology. (Also as 1943 *Tech. Notes natn. advis. Comm. Aeronaut.*, *Washington*, no. 892).

Patnaik, P. C., Sherman, F. S. & Corcos, G. M. 1976 A numerical simulation of Kelvin–Helmholtz waves of finite amplitude. *J. Fluid Mech.* **73**, 215.

Reynolds, O. 1895 On the dynamical theory of incompressible viscous fluids and the determination of the criterion. *Phil. Trans. R. Soc. Lond.* A **186**, 123.

Reynolds, W. C. & Hussain, A. K. M. F. 1972 The mechanics of an organized wave in turbulent shear flow. 3. Theoretical models and comparisons with experiments. *J. Fluid Mech.* **54**, 263.

Roshko, A. 1976 Structure of turbulent shear flows: a new look. *AIAA Jl* **14**, 1349.

Rotta, J. 1951 Statistische Theorie nichthomogener Turbulenz. *Z. Phys.* **129**, 547.

Schubauer, G. B. & Skramstad, H. K. 1948 Laminar boundary layer oscillations and transition on a flat plate. *Rep. natn. advis. Comm. Aeronaut., Washington*, no. 909.

Starr, V. P. 1968 *The physics of negative viscosity phenomena*. New York: McGraw-Hill.

Stuart, J. T. 1956 On the effects of the Reynolds stress on hydrodynamic stability. *Z. angew. Math. Mech.* **36**, S32 (Sonderheft).

Stuart, J. T. 1958 On the nonlinear mechanics of hydrodynamic stability. *J. Fluid Mech.* **4**, 1.

Stuart, J. T. 1963 Hydrodynamic stability. In *Laminar boundary layers* (ed. L. Rosenhead), pp. 492–579. Oxford University Press.

Stuart. J. T. 1965 Hydrodynamic stability. *Appl. Mech. Rev.* **18**, 523.

Tennekes, H. & Lumley, J. L. 1972 *A first course in turbulence*. Massachusetts Institute of Technology Press.

Townsend, A. A. 1976 *The structure of turbulent shear flow*, 2nd edn. Cambridge University Press.

Winant, C. D. & Browand, F. K. 1974 Vortex pairing: the mechanism of turbulent mixing-layer growth at moderate Reynolds number. *J. Fluid Mech.* **63**, 237.

Wygnanski, I. & Fiedler, H. E. 1970 The two-dimensional mixing region. *J. Fluid Mech.* **41**, 327.